The Kinetics and Thermodynamics of the Amyloid Beta Peptide

Lindberg, Max

2024

Document Version:
Publisher's PDF, also known as Version of record

The Kinetics and Thermodynamics of the Amyloid Beta Peptide

MAX LINDBERG

FACULTY OF SCIENCE | DEPARTMENT OF CHEMISTRY | LUND UNIVERSITY

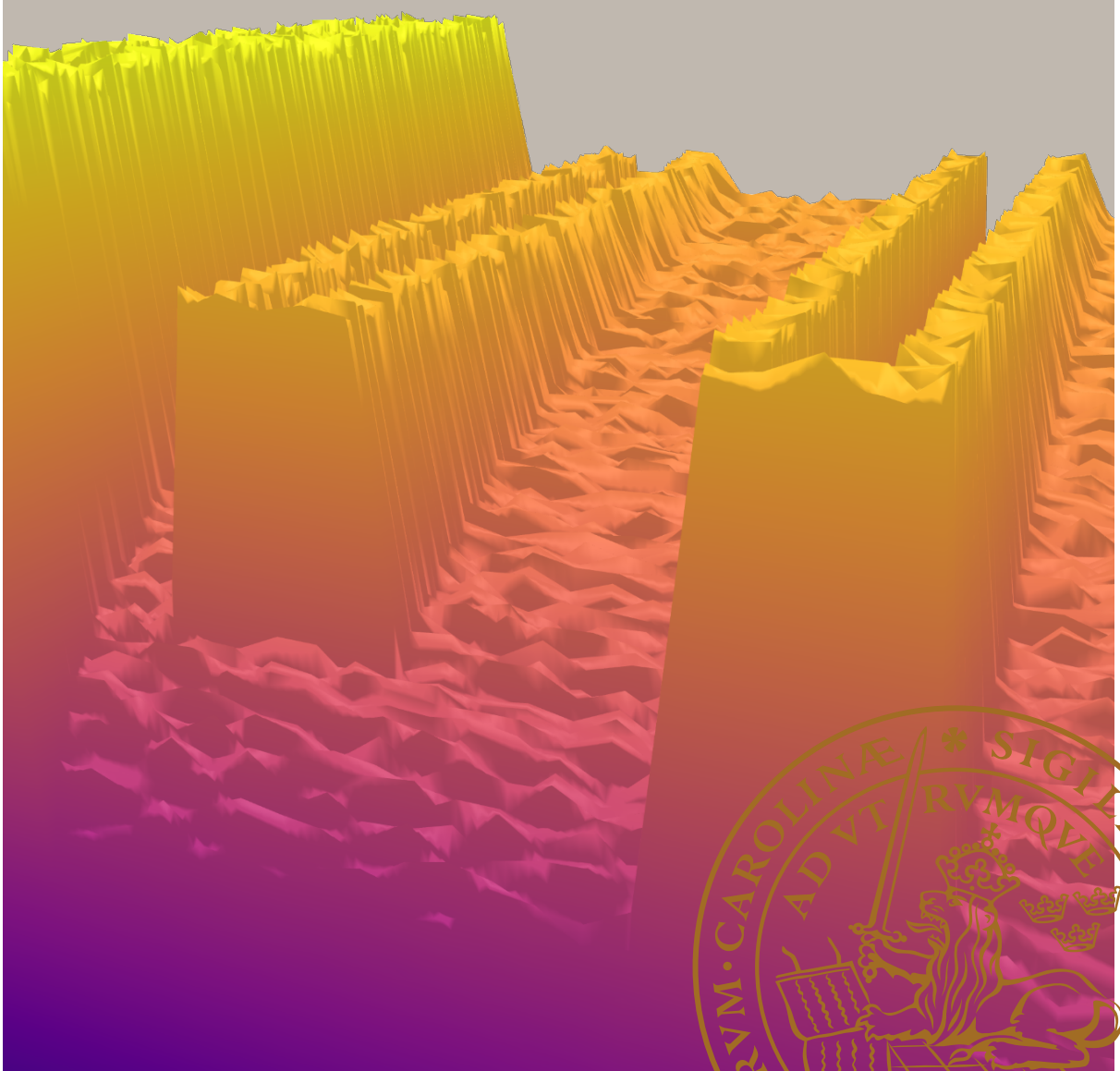

The Kinetics and Thermodynamics of the Amyloid Beta Peptide

The Kinetics and Thermodynamics of the Amyloid Beta Peptide

Max Lindberg

LUND
UNIVERSITY

Thesis for the degree of Doctor of Philosophy
Thesis advisors: Prof. Sara Linse, Prof. Emma Sparr
Faculty opponent: Prof. Daniel Aili

To be presented, with the permission of the Faculty of Science of Lund University, for public criticism in the Kemicentrum lecture hall A at the Department of Chemistry on Friday, 29th of November 2024 at 13:00.

The Kinetics and Thermodynamics of the Amyloid Beta Peptide

Max Lindberg

LUND
UNIVERSITY

Faculty Opponent

Prof. Daniel Aili
Linköping University
Linköping, Sweden

Evaluation Committee

Prof. Pia Ädelroth
Stockholm University
Stockholm, Sweden

Prof. Vito Fodera
University of Copenhagen
Copenhagen, Denmark

Prof. Trevor Forsyth
Lund University
Lund, Sweden

Cover front: A schematic representation of the energy landscape for amyloid formation.
Cover back: QR code leading to https://max-thesis.minimammoths.tech.

Faculty of Science, Department of Chemistry
ISBN: 978-91-8096-074-8 (print)
ISBN: 978-91-8096-075-5 (pdf)

Printed in Sweden by Tryckeriet i E-huset, Lund University, Lund 2024

”Time always seem to move much faster than I do... ” -Max

Contents

List of publications

This thesis is based on the following publications:

1 **A label-free high-throughput protein solubility assay and its application to Aβ40**
M. Lindberg, E. Axell, E. Sparr, S. Linse (2024)
Biophysical Chemistry, p. 107165

2 **The temperature dependence of abeta solubility and it's implications for the thermodynamic driving forces of amyloid formation**
M. Lindberg, E. Sparr, S. Linse (2024)
Unpublished manuscript

3 **The role of shear forces in primary and secondary nucleation of amyloid fibrils**
E. Axell*, J. Hu*, **M. Lindberg***, A.J. Dear, L. Ortigosa-Pascual, E.A. Andrzejewska, G. Šneiderienė, D. Thacker, T.P.J. Knowles, E. Sparr, S. Linse (2024)
PNAS, Vol. 121, Issue 25, p. e2322572121
*these authors contributed equally

4 **Differentiating amyloid morphs by simple ThT-based kinetic assays**
M. Lindberg, D. Thacker, E. Sparr, S. Linse, A.J. Dear (2024)
Unpublished manuscript

Publications not included in the thesis:

1 **Reduced protein solubility - cause or consequence in amyloid disease?**
M. Lindberg, J. Hu, E. Sparr, S. Linse (2024)
QRB Discovery (Accepted manuscript)

Author contributions

The next pages summarize my contribution to each paper included in this thesis.

Paper I:
A label-free high-throughput protein solubility assay and its application to Aβ40

M. Lindberg, E. Axell, E. Sparr, S. Linse (2024)
Biophysical Chemistry, p. 107165

I conceptualized the method, did all the experiments, data analysis and figures included in the paper and wrote a strong majority of the text.

Paper II:
The temperature dependence of amyloid beta solubility and it's implications for the thermodynamic driving forces of amyloid formation

M. Lindberg, E. Sparr, S. Linse (2024)
Unpublished manuscript

I led the experimental design, performed all experiments and data analysis. I also wrote a majority of the text and created all figures.

Paper III:
The role of shear forces in primary and secondary nucleation of amyloid fibrils

E. Axell*, J. Hu*, **M. Lindberg***, A.J. Dear, L. Ortigosa-Pascual, E.A. Andrzejewska, G. Šneiderienė, D. Thacker, T.P.J. Knowles, E. Sparr, S. Linse (2024)
PNAS, Vol. 121, Issue 25, p. e2322572121
*these authors contributed equally

I participated in virtually all experimental design, did experiments both together and independently for the brichos inhibition and monomer concentration dependent parts, performed data analysis (linear regressions for the half-time vs concentration data and generated python code to plot and evaluate the different models for concentration dependent kinetics), made 7 of the 16 figures and had a major role in writing and editing.

Paper IV:
Differentiating amyloid morphs by simple ThT-based kinetic assays

M. Lindberg, D. Thacker, E. Sparr, S. Linse, A.J. Dear (2024)
Unpublished manuscript

I co-designed experiments, performed the experiments, participated in data analysis and wrote a majority of the text and created all figures.

Popular summary

This thesis is centered around two main concepts, solubility and fibril morph.

Solubility is principally quite easy, how much of a substance can you dissolve in a solution? Imagine putting a spoon of sugar in a glass of water, the sugar will fall down to bottom and soon dissolve. However, what happens if you continue to add sugar? After adding about 1 and ¼ dl of sugar per dl of water, it won't dissolve anymore, you have then saturated the solution and reached solubility. After doing such an extreme experiment, you might feel like having a drink. Then you realize that you've basically just done the first step of making syrup. You therefore promptly proceed to boil the solution and voilà! The remaining sugar dissolved. This is because solubility generally increases with temperature. However, an exception to this is presented in Paper II, where the solubility of an amyloid protein increases with both higher and lower temperatures. This behavior can give insights into the driving forces behind amyloid formation. If you then were to let the syrup cool down again, you might notice that the sugar is still dissolved. The solution is now supersaturated and eventually the sugar will crystallize and fall out of solution, but until then the system is so called "metastable", which is another term that play an important role in this thesis. Investigating the solubility of amyloids is, at least practically, more difficult. This is the motivation for the work done in Paper I, which details the development of a solubility assay for amyloids.

The next concept, fibril morph, means the structure of an amyloid fibril and can be explained as a rope. Just as ropes can consist of different materials, amyloids can consist of different proteins, and just as ropes can be twisted or braided with various number of strands, so an amyloid can have various number of filaments twisted in different ways. A part of the fibril morph that is harder to translate to a rope equivalent, is that these filaments are composed of proteins that are folded into a flat structure and then stacked on top of each other. The fold of these proteins when flat and stacked like this, is referred to as the filament fold, and is a term used throughout this thesis. These fibril morphs can thus have either quite similar properties or rather different ones, even though consisting of the same protein. In Paper IV a method to measure these properties is presented.

Paper III is not directly related to the two concepts, but it explores why amyloids form more

quickly with gentle stirring. The answer, continuing with the analogies, can be explained through dandelions. Imagine dandelions are amyloids and stirring is the wind, how could wind make dandelions spread faster? Just as wind carries away the white fluff from a mature dandelion, we found in Paper III that fluid removes newly formed amyloids from various surfaces when it is stirred. Thus, allowing new amyloids to form faster.

What's the relevance of all this? Amyloids are implicated in many of today's incurable diseases, such as Alzheimer's and Parkinson's disease, but although the connection to disease is clear, the exact mechanisms of how these structures are related to the disease remain unclear. In addition to this, amyloids are also worth studying because of their applications in material science.

Populärvetenskaplig sammanfattning

Denna avhandling är centrerad kring två koncept, löslighet och fibrillmorf (på engelska ”fibril morph”).

Löslighet är egentligen ganska enkelt, hur mycket av något kan du lösa upp i en vätska? Tänk dig att du lägger i en sked socker i ett glas vatten, sockret faller ner på botten och om du rör runt lite så har det snart löst upp sig, inget konstigt. Men vad händer om du fortsätter hälla i socker? När du haft i någonstans runt 1 och ¼ dl socker i 1 dl vatten, så kommer det inte lösa upp sig längre, du har mättat lösningen, och koncentrationen socker i det vattnet är därmed sockrets löslighet. Om du efter detta extremt avancerade experiment känner att du behöver en drink, så inser du kanske att du i princip redan är halvvägs till att göra sockerlag och kokar därmed upp vattnet med socker. Helt plötsligt så har allt socker löst sig! Detta är för att löslighet generellt sett ökar med temperatur, ett undantag till detta presenteras dock i Artikel II. Där ökar lösligheten för ett amyloid protein både med högre och lägre temperatur. Vilket kan avslöja de termodynamiska drivkrafterna bakom bildandet av amyloider. Om du sedan låter sockerlagen svalna igen så kanske du blir förvånad över att allt socker fortfarande är löst, detta kallas då att lösningen är övermättad. Så småningom kommer lite av sockret kristallisera ut ur lösningen för att åter nå en mättad lösning. Tills detta sker så är systemet så kallat metastabilt, vilket är ett viktigt begrepp i artikel I. När det kommer till löslighet av amyloider, så blir det, åtminstone praktiskt, mycket svårare. I Artikel I har vi därför utvecklat metodologi för att mäta löslighet av amyloider.

Nästa begrepp, fibrillmorf, är vilken struktur en amyloid har och kan förklaras med hjälp av rep. Du kan göra rep av olika material, på samma sätt kan amyloider kan bestå av olika proteiner. Rep kan vara tvinnade eller flätade av olika många trådar och på samma sätt så kan amyloider bestå av olika många filament som kan vara tvinnade på olika sätt. En aspekt som är svårare att översätta till rep, är att dessa filament består av proteiner som är veckade så att de blir platta och sedan staplas ovanpå varandra. De bildar då filament. Hur denna veckning sker kan spela stor roll för fibrillens egenskaper, därför pratas det en hel del om filamentveckning (”filament fold” på engelska). Dessa fibrillmorfer kan därmed ha antingen snarlika eller välidgt olika egenskaper, trots att de består av samma protein. I Artikel IV presenteras en metod för att mäta sådana egenskaper.

Artikel III är inte direkt kopplat till de två koncepten ovan, utan där undersökte vi istället varför amyloider bildas snabbare vid lätt omrörning. Svaret kan förklaras, om vi nu ska fortsätta med analogier, via maskroser. Tänk att maskroser är amyloider och omrörning är vind, hur skulle vind kunna göra att maskroser sprider sig snabbare? Jo, precis som vinden rycker av det vita på en mogen maskros, så rycker vätskan bort nybildade amyloider från diverse ytor om provet rörs om, det kan då växa fram nya amyloider snabbare.

Varför är amyloiders löslighet och struktur värt att studera? Amyloider är starkt kopplade till många av dagens obotliga sjukdomar, såsom Alzheimers och Parkinsons sjukdom, men det är fortfarande mycket oklarheter kring hur de faktiskt leder till sjukdom och symtom. Utöver detta är amyloider även värda att studera för deras användning inom materialvetenskap.

Acknowledgements

Sara and **Emma** you are the best supervisors a PhD student can wish for! Working under you have meant an incredible freedom to pursue everything I thought were interesting, which truly made this my dream job. I'm constantly amazed at how much time you both have been able to spend on me, and I'm deeply grateful. I hope I'll come close to your levels of balance between lab work, teaching and family life when I "grow up". You're my role models. **Emil**, the guy I started on the same day as, it's been amazing to have someone else going through this journey with me, and the endless discussions about our projects both in the office, at parties and by text late at night has been invaluable. It would not have been the same without you! **Lei**, you're a great office mate (although you set the thermostat too high) and I wanna thank you for all the interesting discussions and for being able to fix any of my figures with just a glance, it's been great to just turn around and ask is this clear? And get exactly why not and how to fix it in response. **Andreas**, you always add an extra dimension to all discussions, it feels like I sometimes learn more from a coffee break with you than I've done in some courses! Your joy for the lab is contagious and seem to only be rivaled by Sara's. It's also nice to have someone so read up on Brandon Sanderson to really nerd out with. **Jing**, for asking questions until you truly understand, more people should follow your example! I thought I knew protein purification, but then I tried to teach you and your questions made me realize how many holes my knowledge really had. **Josef** & **Elin** my master students, I'm both very proud and a little bit guilty for luring you into the frustrating but fascinating field of amyloid solubility, I gained a lot of perspective when trying to explain to you what I've learned and I will follow you both with a keen interest. **Karolina** & **Marija** my dear musketeers, thank you for all the wonderful times! Always being up for a beer, and teaching me essential slav things, like how to make bureks or eat ogórki while in a proper squat and shotting vodka. **Ewelina**, for bringing some well needed "Östgötska" to the group and just being awesome. **Erik** "The guy who knows everything" apparently knows how be an excellent lab police as well, thank you for keeping us in check ;) **Marco**, **Noemi**, **Nicole**, **Timas** and the rest of Phys. Chem., for giving us biochemists a foothold in the cool but scary field of Physical Chemistry. **Dev**, **Tinna**, **Mattias**, **Vero**, **Tanja**, **Kalyani** and **Rebecca** "The OGs", thank you for passing down wisdom and tips & tricks for life as a PhD student in Saras group (and for changing the group meetings from 8.00, that would have been the end of me!). **Katja**, for teaching me everything I know

about MS. It's always such a joy to come down to your lab and your high spirits! **Thom** and **Martin**, for teaching me a lot about instruments and for keeping the lab running. **All past and present members of Sara's group**, for making it a wonderful group to be in with amazing science to build on!

Magnus & **Maryam**, the center-pillars of CMPS that makes all the wheels go round. You're always happy to help and whatever one or the other of you two can't fix, is not worth fixing! You two are a big part of what CMPS feels like a family, thank you! **Helin**, You're always great to talk to whether it's about bullshit or deep stuff. Teaching with you in the course labs sometimes felt more like being back in high-school than working (AVGN..) **Simon B**, we're very different in a lot of ways, which makes hanging out with you extra nice! **Carmen**, I really appreciate all of you AW initiatives. **Theresa**, you're always up for a beer and regardless if I feel on top of world or in the dumps, I always feel better after talking to you! **Rest of the CMPS**, for making KC a wonderful workplace that feels like a home with a huge family.
Julie & **Robbie**, a party always improves when you join, I really wish I would've gotten to know you both earlier!

Abbe, **Henke**, **Jonte**, **Axel**, **Måns**: For more than can be expressed in words, for a wonderful childhood, for the feeling that whatever happens you are there, for the games, the parties and all stupid shit that lead to great stories! **PD**, I've seen you as an academic big brother, from our fun together in iGEM and spontaneous crashing of Skytte-C to sharing an office, you've always been loads of fun and inspired me to follow your footsteps. **Johan**, if PD is my academic big brother, then you're my little brother! You always have a weird and surprisingly valid take, with highlights as "it's all just basically soap" and "why not purify chaperones from fruits?" **Per** and **Sofie**, to continue the analogy, I consider you my academic parents. Thank you so much for bringing me into the world of amyloids, giving me so much freedom and for showing me how beautiful science can be, with everything from hyperspectral microscopy to negative stain TEM. **Zuzanna**, **Katta**, **Marie** and **Elin H** for making the Linköping years as great as they were! (and extra to Marie for keeping me alive during iGEM ;)) **Elin J**, **Sonen** and **Linnea**, for being just wonderful people, I seldom feel as comfortable as when hanging out with you guys and it's always a great party. **Carin** and **Lars**, for providing new perspectives on the world and for excellent breaks from stress and academia, with just the right kind of crazy, whether it's in Ammarnäs, torpet or Leninbadet. **Uno**, **Inga**, **Annvor** and **Krister**, you were a constant source of inspiration and stimulation when I was growing up, I'll never forget all the interesting math problems or the week trying out university as a 15-year old. **Anders** and **Maria**, for all the good times! **All my relatives**, for more than there's space for here, but for old stories, play fights and wonderful days at the summer house to mention a few. **TG**, thank you for dragging me down to Skåne, enabling this whole PhD and for training (ruining?) my language skills by your insistence of using nonsensical words as much as possible. I floff you.

Of course, the acknowledgments to my family could go on for a whole book, but to summarize: **Dad**, you're probably responsible for my tech interest, which is now my biggest hobby. Also it was from you that I learned the power of "just try", if it breaks we'll just fix it (it will probably be a 5 min job, anyway ;)) I think this mindset have served me well in science. **Mom**, for making me who I am and always encouraging me in my pursuit of science, whether it's fluor and water bombs, push-ups as a reward for finishing homework (how did you even figure out that would work??) or encouraging words whenever the PhD pressure peaked. **Maja**, for being the best little sister a guy can wish for! **Colin**, brother, talking with you is like riding a rollercoaster, full of twists and turns and I love every second of it. You're great!

Part I

Research context

Chapter 1

Proteins and their Folding

The word "protein" was coined by Jöns Jakob Berzelius in 1838 based on the greek word "$\pi\rho\omega\tau\epsilon\iota o\varsigma$", meaning "primary", since it was considered to be the primary source of nutrients in food [1, 2]. Since then an enormous amount of time and energy has gone into studying proteins, as they are essential for life and a promising direction for various materials [3, 4].

1.1 Proteins and their Fold

Proteins are dependent on their structure to perform their function, whether this is transporting oxygen in blood, building muscles, catalyze reactions or regulate DNA. Usually this means that the proteins need to fold in a particular way [5] but sometimes it's rather the absence of a defined fold that is the key to their function, as in the intrinsically disordered proteins (IDPs) which may fold first upon binding to targets [6]. The folding of proteins is generally considered to be driven by the hydrophobic effect [7], sometimes also called the hydrophobic interaction [8]. This is a simple phenomenon with complex explanations, it is essentially the reason that oil and water don't mix. In elementary school you might've learned that it's because "like dissolves like", but that's not really an explanation, it's just a general rule. A central theme in explanations is that it's because water forms a cage around non-polar molecules such as oil, which then decreases the entropy of water. Grouping the non-polar, or hydrophobic, molecules together then means a larger cage is formed which, as the area of a sphere increases less than it's volume upon addition of more molecules, leads to fewer water molecules that need to form cages per oily substance and the entropy of water decreases less compared to complete mixing of the oil and water [8]. However, this explanation has been criticized for not fully explaining all aspects of the phenomenon, such as the temperature dependence of non-polar molecules' solubility [9] and remains a controversal topic [10]. Regardless of the explanation, the fact that there is a driving force to hide hydrophobic molecules from water is not under debate. Thus, if you

have a long sequence of amino acids where some are charged, some polar and some apolar, the hydrophobic effect will lead to most of the apolar residues being hidden in the interior, while the more polar and charged amino acids are exposed to the water. A reasonable question then, is how hydrophobic or hydrophilic are the different amino acids? This is a surprisingly contended issue depending on which property lies behind the ranking and several different scales have been published, a few of which are summarized in Figure 1.1. These scales can be based on the solubility of the amino acids in different solvents [11], how solvent accessible the amino acids usually end up in proteins [12], theoretical calculations [10, 13] or be a consensus of several previously published scales [14–16].

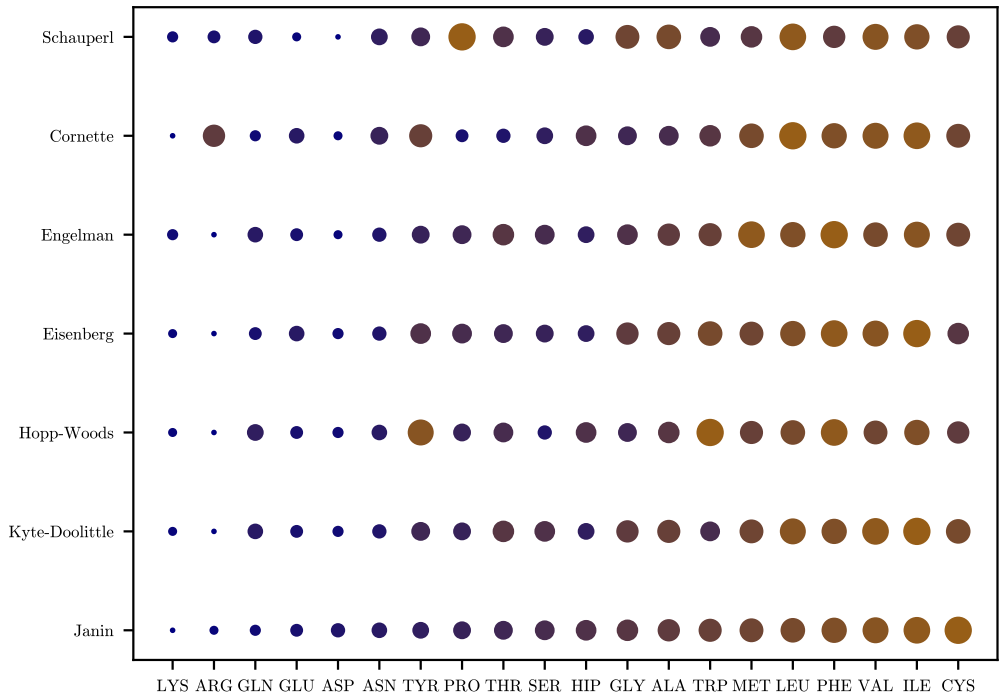

Figure 1.1: Seven different hydrophobicity scales for the 20 natural amino acids in chronological order (Janin [12],Kyte-Doolittle [14], Hopp-Woods [11], Eisenberg [15], Engelman [13], Cornette [16], Schauperl [10]) and all are sized (small to large) and colored (blue to bronze) according to their ranking (hydrophilic to hydrophobic). HIP is the protonated and postively charged version of histidine.

Chapter 2

Amyloids

Amyloid fibrils consist of one or more protofilaments, which in turn are stacks of proteins in β-sheet structure [17]. Although made of protein, they get their name from the greek word "amylon" which means starch, since they were initially believed to consist of starch, based on histological iodine staining [1] [18]. While amyloids were discovered already in the 1800's, the first case of Alzheimer's disease was reported in 1906 by Alois Alzheimer after a 50 year old man had presented symptoms of senile dementia and upon death had the typical plaques usually only seen in old people. When a colleague of his four years later included the case in a book, it was dubbed "Alzheimer's disease" [19]. Then 78 years later, in 1984, Glenner and Wong discovered that the plaques characteristic for the disease consisted of primarily a small peptide, which they named "amyloid fibril protein β" [20] which later became "amyloid beta", "abeta" or "Aβ". After this, amyloids became a very active area of research, see Figure 2.1. However, people soon realized that reproducibility when working with amyloids is a fleeting thing and that minute differences in experimental set-ups can lead to big changes in aggregation kinetics [21, 22], nicely exemplified by Aβ getting the moniker *"the peptide from hell"* [23]. Luckily, the reproducibility of Aβ kinetics were mostly tamed in 2010 by Hellstrand et al. [24], which lead to insights about the mechanisms behind aggregation, including the role of secondary nucleation [25]. While the field of amyloid formation kinetics (aiming to find the speed and mechanism by which it aggregated) quickly grew, the other side of the coin, it's thermodynamics (i.e. the driving forces behind amyloid formation), has remained comparatively understudied [26]. Another major hallmark with great importance for structural investigations of amyloids is the "cryo-EM revolution", where researchers overcame some key hurdles in order to successfully use electron microscopes for biomolecules in the 1980s, which enabled structural studies of more biomolecules than possible with nuclear magnetic resonance (NMR) or X-ray diffraction. Since then the possible resolution acquired has just increased and increased due to improved microscopes, better software and more powerful computers. Today it is possible to get atomic resolution mod-

[1] Although some people preferred the term "lardaceous" because of it's similarity in appearance to bacon.

els of biomolecules, and the researchers behind the key advances enabling this achievement were awarded the Nobel prize in chemistry in 2017 [27]. Coincidentally this was the year the first high-resolution models of amyloid structures by cryo-EM started to appear [28, 29]. While excellent structural models of amyloid fibrils have been produced before 2017 by other methods, such as solid state NMR [30], the speed with which new structural models can be solved increased exponentially with cryo-EM and today >475 models of amyloid structures have been presented (https://people.mbi.ucla.edu/sawaya/amyloidatlas/), with one example shown in Figure 2.2.

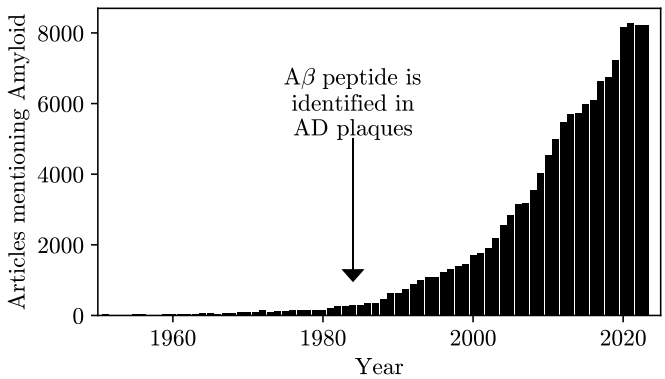

Figure 2.1: Number of search results per year containing the word "Amyloid" on pubmed up until 2024. AD is Alzheimer's disease.

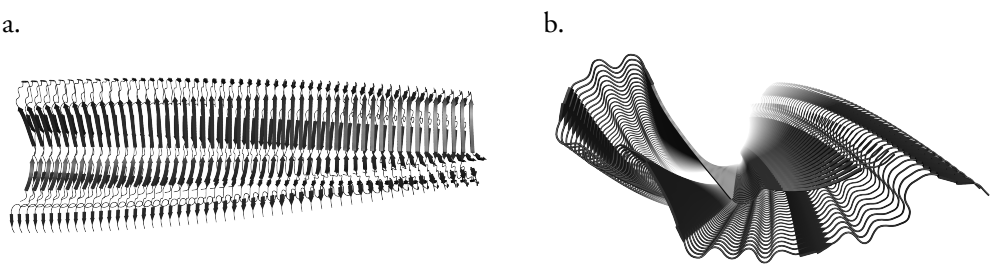

Figure 2.2: An amyloid fibril viewed from the side (a.) and from the top (b.), where arrows represent β-strands. This image was generated through CreateFibril v2.5 [31] and PyMol [32] using the PDB entry 6QJH, which is a structural model of full length tau (2N4R) that has formed fibrils in the presence of heparin [33].

2.1 Thermodynamics of Amyloids

So why do proteins form this particular structure? Well, as can be seen in Figure 2.2, amyloids consist of many proteins folded in a particular and identical way and stacked on top of each other, i.e. it's a coupled folding and assembly reaction. However, in contrast to most protein folding processes, amyloid formation involves so many subunits that it has the characteristics of a phase transition, where dilute monomers in solution go together and form a pure solid phase with crystalline packing [24, 34, 35]. The perspective of fibrils as one-dimensional crystals in equilibrium with protein monomers in solution will be important throughout this thesis, therefore I will here go through some of the underlying thermodynamics.

The chemical potential for a solute in solution is $\mu = \mu^\circ + RT\ln(a)$, where μ° is the standard chemical potential (i.e. the chemical potential at a standard state, usually 1 mol/l), R is the universal gas constant (8.314 J K^{-1} mol^{-1}), T is the absolute temperature in K and a is the activity of the solute. This activity can be seen as an effective concentration and is defined as $a = \gamma c/c^\circ$ where γ is the activity coefficient, c is the concentration (in mol/l) and c° is the standard concentration, e.g. 1 mol/l. As γ goes towards 1 when c goes towards 0 and we usually work with protein concentrations on the order of 10 µM (which corresponds to 0.000018 % of the number of molecules present), we can safely assume that γ is very close to 1 and then the expression for the chemical potential of protein monomers in solution becomes $\mu_m = \mu_m^\circ + RT\ln(c)$. For monomers in the fibrils, the expression for the chemical potential is easier, since the activity is 1 for a pure one-component phase, the expression becomes $\mu_f = \mu_f^\circ + RT\ln(1) = \mu_f^\circ + RT\cdot 0 = \mu_f^\circ$, where we choose to define μ_f° as the chemical potential of monomer in fibril at equilibrium, i.e. the most energetically favorable fibril morph possible. At equilibrium, the chemical potential of each component has to be the same in all phases. Thus, we can make an expression for the solubility, s, of the solute, which corresponds to the concentration of monomers in solution at equilibrium with fibrils Eq. 2.1 [8].

$$s = \exp\left(\frac{\mu_f^\circ - \mu_m^\circ}{RT}\right) = \exp\left(\frac{\Delta\mu^\circ}{RT}\right) \tag{2.1}$$

Now , we can raise the question, what happens if the same protein may form different amyloid structures (morphs)? Probably the respective μ_f would differ, since they will fold and assemble in more or less energetically favorable configurations. If energetically less favorable morphs are kinetically favored, this leads to metastable systems with apparent solubilitites higher than true solubility. Sometimes the nucleation barriers are so similar that chance determines which morph(s) or morph distribution initially form, but with time the fibrils will change into a the more energetically favorable morph [36]. This type of behaviour is schematically illustrated in Figure 2.3, where the chemical potential of monomer is plotted and compared to that of three distinct fibril morphs which each give a different solubility,

where at most one can be the most stable one with lowest solubility and the others are less stable with higher apparent solubility.

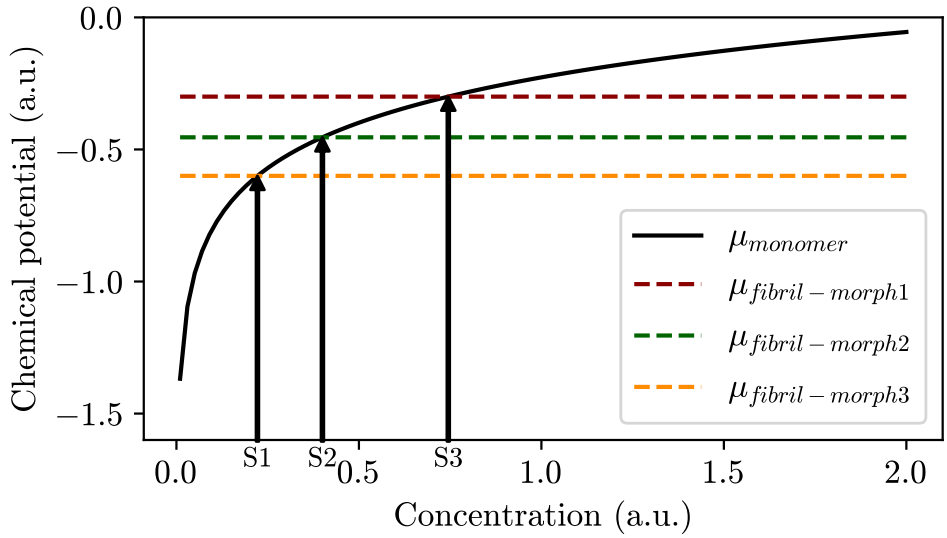

Figure 2.3: Schematic illustration of metastable morphs giving apparent solubilities. The chemical potential of the free monomer is given by $\mu_m = \mu_m^\circ + RT\ln(c)$ with an arbitrary value for μ_m° and the chemical potential for monomer in fibril is given by $\mu_f = \mu_f^\circ + \Delta\mu$, with $\Delta\mu$ being the difference in chemical potential per monomer between a given morph and the most energetically favorable one possible (μ_f°). S1, S2, and S3 represent the apparent solubilities of these three theoretical morphs.

2.2 Master Equation of Amyloid Kinetics

In applications towards the development of disease-modifying drugs, it is not enough to know why amyloids form, one also need to understand the molecular details of how they form. In the early 2000s it was realized that in many cases of amyloid formation, a secondary process in addition to primary nucleation and elongation was needed to explain the fibril formation kinetics [37–39]. This secondary process can be either fragmentation, where fibrils break apart and expose extra ends for elongation, or secondary nucleation, where nucleation of new fibrils is catalyzed by the fibril surface [35, 40]. An overview of the microscopic processes involved in amyloid formation can be seen in Figure 2.4.

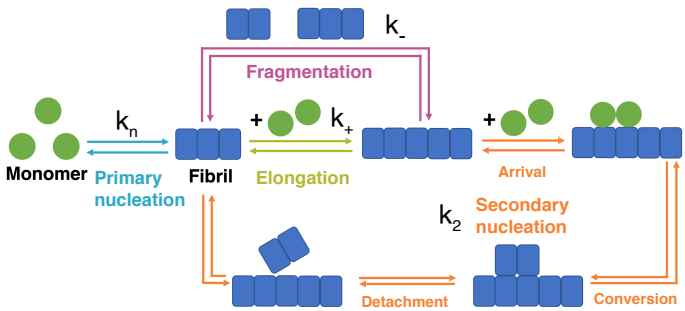

Figure 2.4: A schematic overview of the microscopic processes involved in amyloid formation, taken from Paper III. Secondary nucleation (orange) can be further subdivided into arrival, conversion and detachment steps. Figure is reproduced unaltered from Axell et al. [41] and is under a CC BY-NC-ND 4.0 license.

An important step in the study of amyloid formation mechanisms was the first analytical master equation of fibril formation, published by Knowles et al. in 2009 [42]. A year later, the study of amyloid kinetics for the Aβ peptide became much more reproducible by identifying and removing several sources of irreproducibility [24]. This enabled more systematic studies of fibril formation mechanisms and lead to, among others, a demonstration that shaking the samples during the fibril formation leads to a fragmentation dominated process, while for more quiescent conditions the process is dominated by secondary nucleation [25]. While there have over the years been many mechanistic models proposed to describe the growth of fibrils [43–45], one of particular importance is described by Equation 2.2, which combines elements from earlier models to describe the different microscopic processes. This equation was solved in a range of closed form rate equations by Cohen et al. in 2011, despite it's non-linear nature which made it notoriously hard [46, 47]. Equation 2.2 describes how the concentration of aggregates $f(t, j)$ of size j monomers changes with time t. Each part of Eq. 2.2 (here on a separate line) accounts for one microscopic step, in the following order: elongation, dissociation, fragmentation, primary nucleation and

secondary nucleation. The corresponding rate constants are: k_+, k_{off}, k_-, k_1 and k_2. All steps except dissociation and fragmentation depend on the free monomer concentration $m(t)$. The nucleation steps both have monomer reaction orders (n_1 & n_2) and depend on δ which is 1 if the subscript variables are equal and 0 otherwise.

$$\begin{aligned}\frac{\partial f(t,j)}{\partial t} = \\ 2k_+m(t)f(t,j-1) - 2k_+m(t)f(t,j) \\ +2k_{\text{off}}\, f(t,j+1) - 2k_{\text{off}}\, f(t,j) \\ +2k_- \sum_{i=j+1}^{\infty} f(t,i) - k_-(j-1)f(t,j) \\ +k_1m(t)^{n_1}\delta_{j,n_1} \\ +k_2m(t)^{n_2}\delta_{j,n_2} \sum_{i=n_1}^{\infty} if(t,i)\end{aligned} \tag{2.2}$$

The closed form rate equations to Eq. 2.2 greatly facilitated the estimation of rate constants for the different microscopic steps involved in amyloid formation and lead to a widely used online fitting tool called "Amylofit", developed by Meisl et al. [48]. Subsequently the closed form of the master equation was further optimized, first by Michaels et al. in 2016 [49] and then by Dear et al. in 2020 [50]. The latter is shown in Eq. 2.3, where the symbols have the same meaning as in Eq. 2.2 with the addition of m_{tot} which is the total monomer concentration (i.e. both free monomers and monomers in fibrils). K_P, K_S and K_E are saturation constants for primary nucleation, secondary nucleation and elongation, respectively. At initial monomer concentrations far below saturation concentrations $k'_x \to k_x$.

$$\begin{aligned}\frac{M(t)}{m_{\text{tot}}} = 1 - \left(1 + \frac{\epsilon'}{c'}(e^{\kappa' t} + e^{-\kappa' t} - 2)\right)^{-c'} \text{ where :} \\ \epsilon' = \frac{k'_n m_{\text{tot}}^{n_c}}{2k'_2 m_{\text{tot}}^{n_2+1}},\ \kappa' = \sqrt{2k'_+k'_2 m_{\text{tot}}^{n_2+1}},\ c' = \frac{3}{2n'_2+1} \text{ and :} \\ k'_n = k_n\frac{\mathrm{K}_P^{n_c}}{1+\mathrm{K}_P^{n_c}},\ k'_2 = k_2\frac{\mathrm{K}_S^{n_2}}{1+\mathrm{K}_S^{n_2}},\ k'_+ = k_+\frac{\mathrm{K}_E}{1+\mathrm{K}_E}\end{aligned} \tag{2.3}$$

An equation like 2.2 or 2.3 can then be fitted to experimental data of fibril mass vs time, preferably at several different initial monomer concentrations, which gives estimates for the values of the different rate constants. This may provide insights about the relative

importance of the microscopic steps detailed in Figure 2.4. As an example, adding different antibodies, investigated for treating Alzheimer's disease, as concentration series and performing kinetic analysis as described above showed which microscopic process each antibody affected [51]. The one that inhibited secondary nucleation (aducanumab) was the first disease modifying drug toward Alzheimer's disease ever approved [52], highlighting that kinetic modeling could indeed be a powerful tool. For a sense of how the different microscopic processes affect the overall growth of fibril mass, one may model what would happen if each of the rate constants would be individually decreased or increased by a factor of 10 or 100 [53, 54].

As mentioned, the modeling requires measures of fibril mass over time, which may be monitored via CD spectra, filter trap assays, intrinsic fluorescence or on the florescence of dye molecules such as luminescent oligothiophenes (LCOs), 8-Anilino-1-naphthalenesulfonic acid (ANS) or Thioflavin T (ThT) [53, 55], depicted in Figure 2.5 [45, 56]. While the exact binding mode of ThT remains controversal [45] it binds to most amyloids and goes from nearly non-fluorescent to strongly fluorescent upon binding to the amyloid in a manner proportional to fibril mass, at least in a validated concentration range [57]. However, ThT binding and subsequent fluorescence have been reported to depend strongly on the fibril morph [36, 58], which could be due to either different binding modes that provide different chemical environments and restrict the rotation of ThT to different extent [45] or just a matter of binding affinity.

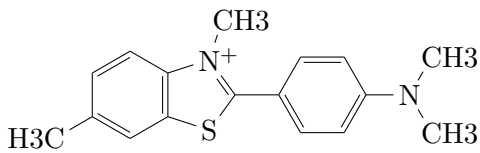

Figure 2.5: Structure of ThT [59]

2.3 Relevance of Amyloids outside of Pathology

Another point worth highlighting with amyloids is that they may play an important role for the fundamental understanding of protein folding in general. As a field, we've had a huge breakthrough the last few years with the development of AlphaFold[1] [61] which is exceptional at predicting protein structures, but it is quite heavily based on evolutionary trends (i.e. which amino acids are usually close to each other in this type of sequence), this evolutionary basis might be why it still predicts amyloid structures poorly [62]. With the recent avalanche of structural models of amyloids and the ever increasing computational power at our disposal, these proteins that can form a multitude of extremely stable struc-

[1]The development of which lead to one half of the Nobel prize in chemistry 2024 [60]

tures under ever so slightly different conditions might be important to further improve protein prediction tools, such as AlphaFold.

Finally, amyloids don't have to be something bad, they are actually very promising candidates in materials science [63–65] with applications ranging from self-assembling conducting nanowires [66] to plant-based plastic alternatives [67] and hydrogels for 3D cell cultures [68]. Some amyloids might even sober you up after a hard night of partying some day in the future, as researchers have developed an amyloid-based hydrogel with dispersed iron atoms that catalyze the alcohol oxidation to acetic acid, with promising results in mice [69].

Chapter 3

Developed Methodology

My work these last four years have mostly been focused on methodology development, i.e. figuring out how to use combinations of existing methods, in order to better answer scientific questions related to amyloid aggregation and amyloid protein solubility. Therefore, this section describes some of the methods I've worked with and how they relate to my particular applications.

3.1 General Considerations Working with Abeta

As mentioned in chapter 2, the Aβ peptide is not easy to handle. However, a huge effort was done by Hellstrand et al. in 2010 [24] to identify factors that helped with reproducibility, which can be summarized as: minimize the air-water interface (e.g. use degassed buffers, pipette carefully to not introduce bubbles and use half-area wells), use non-binding surfaces to not loose protein or accelerate nucleation (such as PEG-ylated plates[1]) and finally, to work with extremely pure peptide samples and use filtered buffers with analytical grade chemicals. If the peptide is purified from recombinant expression in *E. coli* through inclusion bodies, with one ion-exchange chromatography step using diethylamine (DEAE) and three size exclusion chromatography (SEC) steps at high pH, it can reach purities of 99.99 % [71]. The last one of those SEC steps should be right before an experiment to ensure monomeric peptide. This is the established procedure in our lab, and inspired by this, we have tested most of the remaining surfaces that the peptide comes into contact with in the different methods that I've used and found that, while you do lose some protein in tubes, this is within experimental errors (at least when handling concentrations of 500 nM), Figure 3.1a. However, the loss is more substantial when pipetting, as shown in Figure 3.1b. Thus, avoiding sample handling as much as possible when working with low concentrations of Aβ has been a priority of mine.

[1]Polyethylene glycol (PEG) seem to be among the few surfaces where Aβ does not adsorb at all [70].

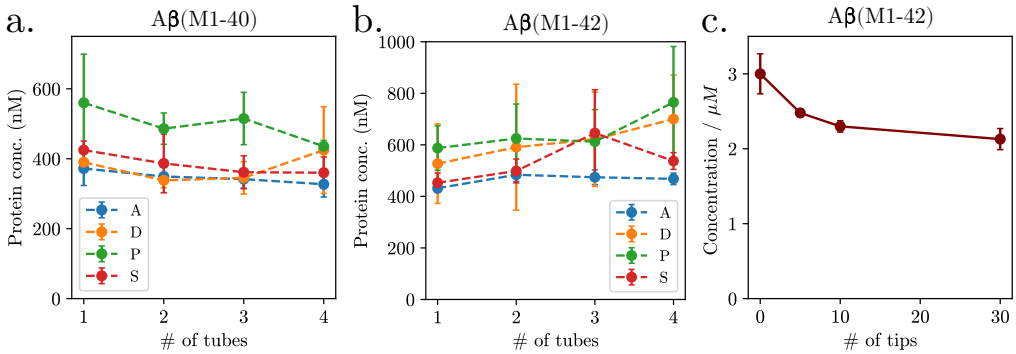

Figure 3.1: Protein concentration as a function of surface exposure for Aβ(M1-40) (a.) or Aβ(M1-42) (b. and c.). The surface is either of microcentrifuge tubes (a. and b.) of type and vendor A: Maxymum recovery tubes (Axygen, blue markers), D: DNA LoBind tubes (Eppendorf, orange markers), P: Protein LoBind tubes (Eppendorf, green markers), S: untreated tubes (Sarstedt, red) or of untreated pipette tips (c.). N=3 and error bars represent standard deviation.

3.2 Quantification of Monomers

The absolutely most common method of protein quantification is by UV absorbance and Beer-Lambert's law, $A = \epsilon c l$ where A is the absorbance, ϵ is the molar absorption coefficient, c is the concentration and l is the path length [8]. This method is convenient and non-invasive but it has the drawback that it is nonspecific, meaning that the absorbance of all buffer components in the sample need to be subtracted. Furthermore, the method only works properly for samples with high protein purity and lack of light scattering, although the contribution of this can be estimated from the wavelength-dependence of the baseline. Since we always purify our monomer with a SEC step right before every experiment, we can get a good estimate of the concentration by integrating the absorbance at 280 nm of the collected peak in the chromatogram and using Beer-Lambert's law with a molar absorption coefficient of 1440 $M^{-1}cm^{-1}$. With proper baseline subtraction this is a reasonably reliable protein quantification method. However, to measure solubilities as low as 20 nM, we can't just put it through the SEC again, since you both lose ca 50 % of all Aβ in each SEC step [71] and since 20 nM peptide with a ϵ of 1440 $M^{-1}cm^{-1}$ gives too low absorbance to be measured. Therefore we turned to high performance liquid chromatography (HPLC) coupled with a very sensitive absorbance detector and a connected single quadropole mass spectrometer (qMS).

3.2.1 HPLC-MS

An HPLC is principally just a pump[2] that pushes a liquid (mobile phase) through a porous material (solid phase) in a column. Usually with one or more detectors downstream of the column. This means that if a sample is mixed in with the mobile phase, it will enter the column and the components in the sample will interact differently with the solid phase based on their molecular properties, which can be e.g. size or hydrophobicity. In my work I've been using a reverse phase column with a hydrophobic solid phase, which means that the molecules in the sample spend more time in the solid phase the more hydrophobic they are. To facilitate this separation, we can gradually change the mobile phase to something less polar, which will change the partitioning of the molecules from the solid into the mobile phase to enter the detector(-s). The most common way of doing this is by starting with an aqueous solution and then gradually increasing the percentage of the apolar solvent acetonitrile (ACN). Luckily, no monomer seems to adsorb to any surfaces in our HPLC system, as the calculated amounts of Aβ from the area of the peaks in the chromatograms match very well with the injected amounts, Figure 3.2. To improve our sensitivity, we go down in wavelength to 205 nm, where instead of only tryptophans, tyrosine and phenylalanines, all the peptide bonds between amino acids can absorb light and our signal for Aβ is amplified by a factor of 118 [72] (absorption coefficients at 205 and 214 nm from protein sequence can be calculated at https://bestsel.elte.hu/extcoeff.php).

Single Quadropole Mass Spectrometer

After the absorbance detector we have a single quadropole mass spectrometer (qMS), which ionizes the eluted molecules by a high voltage (4.5 kV in our case) upon which they fly in between 4 poles. These poles create an electric field which deflects all molecules except those with a certain mass-to-charge ratio (m/z), the molecules then hit a detector and get registered as counts. By then changing this electric field thousands of times per second, we can get spectra detailing which mass-to-charge ratios elute at which times. Another possibility is to set the field to a certain fixed value and monitor for specific compounds [73]. Thus, with the addition of a qMS, we get more information about which molecules elute at any given point, as well as an orthogonal quantification method, which is at least as sensitive as the UV-absorbance at 205 nm, see Figure 3.3.

3.2.2 O-pthalaldehyde (OPA)

As can be seen above, an HPLC-MS is great, being both selective and sensitive, which is why it is one of the most widely used analytical techniques [73]. However, in my developed HPLC protocols each sample takes 15 minutes to run, which is not a lot of time but for hundreds of samples it becomes a lot. Also HPLC-MS systems are expensive. So in

[2]A very very good pump though, that can give a steady flow with ca. 1000 bars of back pressure.

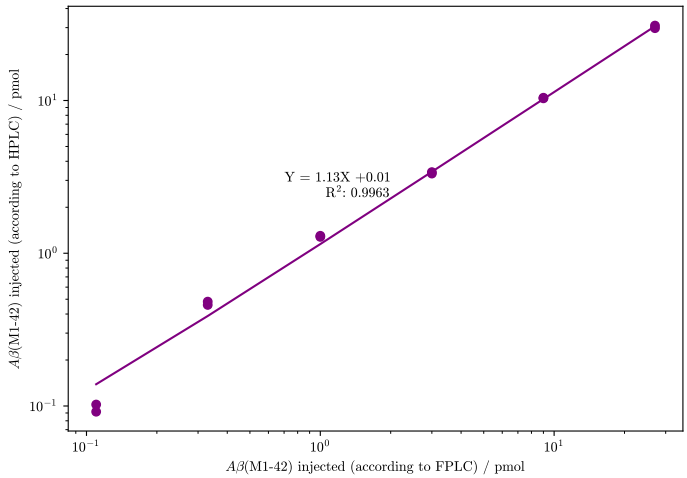

Figure 3.2: Evaluation of HPLC quantification where a known amount of Aβ(M1-42) is injected into the HPLC system and the amount that comes out is calculated based on integration of the absorbance at 205 nm of the corresponding peak in the chromatogram. Linear regression is done with a weighting of 1/C, where C is the peptide concentration, N=2.

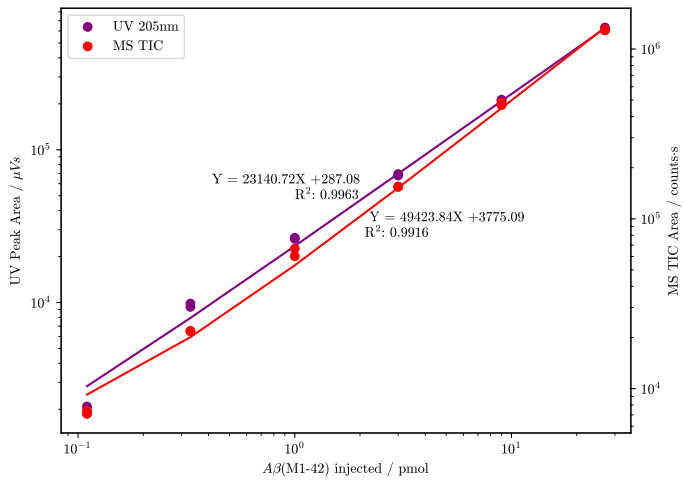

Figure 3.3: Standard curves for HPLC-MS quantification of Aβ(M1-42) with chromatogram peak areas from either 205 nm absorbance (purple, left y-axis) or the total ion current (TIC) from monitored Aβ(M1-42) ions (red, right y-axis). Linear regression is done with a weighting of 1/C, where C is the peptide concentration, N=2.

order to have a more accessible and high-throughput alternative, we investigated fluorescent microwell plate assays. While there are plenty of fluorescent molecules that can be conjugated to proteins, most are fluorescent on their own, which introduces two problems. Either you need to perform the whole experiment with the labeled protein, which then has different properties compared to the unmodified protein of interest, or you need to label it afterwards and wash away all unbound probe. Both of these approaches present problems if you want to quantify nanomolar levels of a sticky peptide. However, there are a also some molecules that become fluorescent first upon reacting with the protein. One such molecule is called o-pthalaldehyde (OPA) [74, 75]. OPA reacts covalently with primary amines according to the reaction mechanism in Figure 3.4. In an assay that relies on OPA florescence, it is enough to add the OPA solution to a protein sample and within minutes it will be strongly fluorescent. The fast reaction times and lack of sample preparation enables convenient quantification of a whole 96-well plate within minutes. While not as sensitive and robust as the HPLC-MS, the method is linear over 3 orders of magnitude and give reliable quantification down to 40 nM Aβ, see Figure 3.4. The big drawback with the OPA-based assay presented in Paper I though, is that OPA reacts with all primary amines, so it has very high requirements on the purity of the sample. This general reactivity also means that in order to quantify the monomer concentration in equilibrium with fibrils, the fibrils must first be removed.

3.3 Reaching Equilibrium

The conceptually most straightforward way to measure solubility is to stepwise add and dissolve the solute until no more solute can be dissolved and it precipitates, then the concentration right before that is the solubility. However, the time it takes for amyloids to precipitate increases exponentially with the inverse initial monomer concentration [24], meaning that one can reach situations where monomer concentration in the solution by far exceeds the monomer solubility. The solution can remain supersaturated over an extended period of time, i.e. it's metastable over that time [78]. Therefore, we need to take another approach to experimentally obtain measures of the solubility. As discussed in section 2.1, solubility is the monomer concentration that can co-exist with fibrils at equilibrium. Such an equilibrium can in principle be achieved in two main ways, either by starting with an excess of monomer (supersaturation) that forms fibrils until the driving force to do so is gone, or by starting with fibrils at a monomer concentration below solubility (undersaturation) so that the fibrils will dissolve until the solution is saturated with monomers. Since the dissolution of Aβ fibrils appears to be very slow, we have focused on going from supersaturated solutions. If the initial monomer concentration is high enough, fibrils will form in an experimentally reasonable time [24, 78]. However, if the monomer concentration is too high the peptide might instead form other morphs with higher apparent solubilities [79, 80] or even amorphous aggregates [81]. Therefore we set up concentration series from 25 μM to 20 nM and let them incubate for various times. This approach have two main

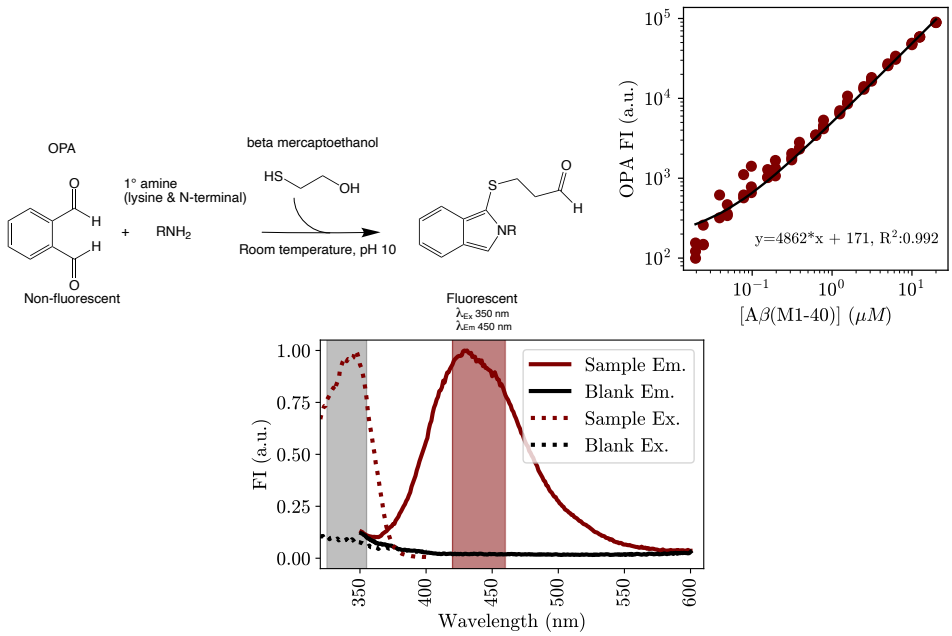

Figure 3.4: Top left: Reaction mechanism for OPA [76]. Top right: the fluorescence intensity (F.I.) response after 5 µl OPA (ref.26025 Thermo scientific) have reacted with 80 µl Aβ(M1-40) at different concentrations for 20 min. Quantification under these conditions are reliable between 40 nM and 20 µM. Bottom: Fluorescent spectra of OPA before (black) and after (red) reaction with protein with shaded areas indicating the excitation (gray) and emission (red) filter settings we found optimal for our applications. Figure adapted from Paper I [77] (CC-BY 4.0)

advantages. First, reaching the same solubility from different initial concentrations and observing it remaining constant over time is strongly indicative that equilibrium actually has been reached, see Figure 3.5. Second, incubating such concentration series will, if covering a wide enough concentration range, provide a built-in standard curve for quantification.

3.4 Separation of Fibrils and Monomers

If the approach to determine solubility is the quantification of monomer in solution at equilibrium with fibrils, one either need a method that selectively measures only monomers in solution or a method which relies on that one first removes the fibrils.

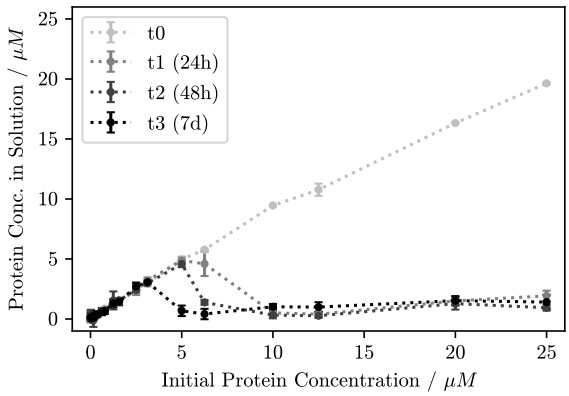

Figure 3.5: Aβ(M1-40) reaching equilibrium from several concentrations and incubation times. Note how 3 µM is still seemingly fully monomeric after 7 days, when the solubility at these conditions is 0.2 µM (Paper I).

3.4.1 Centrifugation

The most common way to separate fibrils from monomers is by centrifugation, where the large fibrils sediment to the bottom while the monomers stay dispersed in the tube. A major advantage of this approach is the minimal sample handling involved, since you can do the separation in the same tube that the fibrils were formed in and then pipette the supernatant to a PEG-ylated microwell plate for concentration determination by either OPA or HPLC-MS. However, there is quite inconsistent information in the literature on how much centrifugation is needed to sufficiently pellet fibrils, with everything from 2000g for 20 min being reported as enough to 250,000g for 110 min being needed [82–86]. What "sufficiently" means is of course depending on your application and the time required in a certain rotor at a certain speed can be calculated if the sedimentation coefficient of the fibrils is known. Although most fibrils will sediment even with no centrifugation, there is still a risk of having some fibrils or fibril fragments dispersed in solution even after centrifugation, which will influence the quantification of monomers. This effect may also differ between different fibril morphs and solution conditions, thus introducing an uncertainty to the quantification method. We've therefore investigated the efficacy of centrifugation for the removal of Aβ fibrils, but with inconclusive results. For this reason, we decided to use other approaches than centrifugation when possible. However, for the studies performed in Paper II we did need to use it as a separation method and there we form fibrils extremely similar to Arosio et al. [87] who found the fibrils to have sedimentation coefficients of 300 S and upwards. We can then model how long it would take to pellet those fibrils in our particular centrifuge by using the equation $t = k/S$, where t is the time (expressed in hours) that it would take to pellet a particle of sedimentation coefficient S (expressed in svedberg),

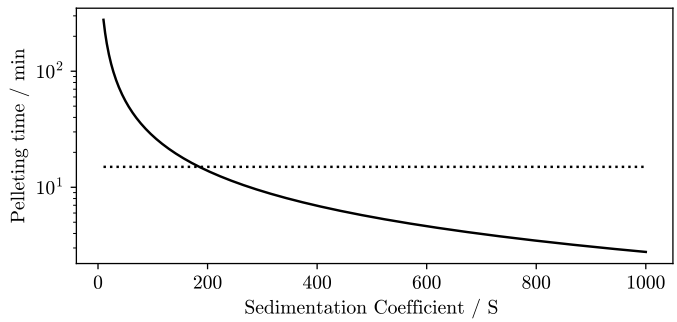

Figure 3.6: The calculated time it would take for a particle to move from the top of the solution to the bottom (pelleting time) in a rotor with a radius of 87 mm spinning at 18000 RPM, assuming a sample height of 5 mm, based on their sedimentation coefficient. Calculated by $t = k/S$ where k is given by Eq. 3.1.

given a clearing factor k, which depends on the dimensions and speed of the centrifuge [88]. To calculate k, we can use equation 3.1, where the distance from the center of the rotor to the top and bottom of the sample is the r_{min} and r_{max}, respectively, and the RPM is the revolutions per minute [88]. All centrifugations were done for at least 15 minutes, which is marked in the figure as a dotted line, showing that it is very likely that virtually all fibrils have been pelleted under these particular conditions. It should be noted though, that temperature affects the pelleting time but is not included in the present modeling. Here centrifugations were performed at 16 °C and I have assumed that the sedimentation coefficients reported by Arosio et al. [87] were determined at room temperature, which is similar enough for the conclusion to hold.

$$k = \frac{2.53 \cdot 10^5 \times \ln(r_{max}/r_{min})}{(\mathrm{RPM}/1000)^2} \tag{3.1}$$

3.4.2 Filtration

The above mentioned uncertainties with centrifugation, as well as the risk of stirring up the pellet by pipetting, made us to instead investigate 96-well filter plates. These have the format of regular 96-well plates but with a filter in the bottom of the wells, through which the samples can be pulled either by applying a vacuum underneath or by centrifuging. This means that if the holes of the filter are small enough to not let through any fibrils, while at the same time the adsorption of monomers to the filter material is sufficiently low, this method would be advantageous for high-throughput separation of monomers from fibrils. We therefore investigated GHP filter plates with a filter size of 200 nm (ref. 8082 PALL) to separate Aβ(M1-42) fibrils from monomers, and compared to previous studies using sim-

ilar approaches [89]. Since the amyloid formation reaction can be extremely sensitive to seeding, and indeed as little as 0.64 nM monomer equivalents of seeds have been reported to give clear effects on the kinetics of Aβ(M1-42) [90], we decided to test the efficacy of the filter plates by performing kinetics with either filtrate from fibrils or buffer. If then fibrils equivalent to 0.64 nM monomers or more would get through the filter, this would cause a clearly visible difference in the kinetics of these two samples, which we do not see, Figure 3.7. We can thus conclude that very little, if any, fibrils pass through the filter.

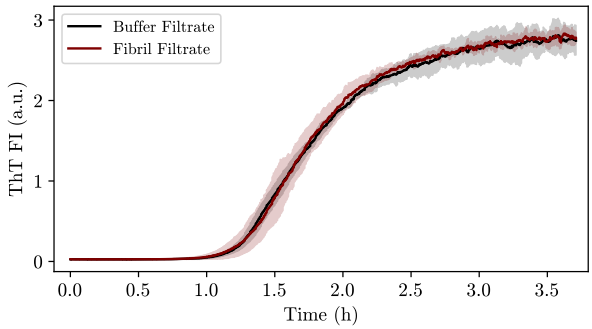

Figure 3.7: Aβ(M1-42) fibril formation kinetics monitored by ThT in filtrate from either buffer or a 10 μM fibril solution (monomer equivalents). Filter was a GHP filter plate (8082, PALL). The curves represent means and the shaded area represents standard deviation, N=4.

As for adsorption of monomer to the filter, this was tested by making concentration series of both Aβ1-40 and Aβ(M1-42) and then measuring the peptide concentration using the OPA assay either with or without the filtration step (Figure 3.8). We do see that the concentration series made from the filtered samples does have a slightly lower slope compared to the corresponding samples from non-filtered samples, but the difference is still within the experimental error. From this we concluded that the filter does not adsorb any significant amounts of monomers.

3.5 Achieving Elongation-Dominated Kinetics

In paper IV we compared elongation rates of Aβ fibril formation. A complication in these studies is that the reaction is also governed by secondary processes [25]. One way would have been to perform global fitting to concentration dependent kinetics, using equations like the ones described in section 2.2, which can then give good estimates of the different rate constants [91]. However, we wanted to turn the process into a convenient assay that limits the number of samples required. Therefore, we investigated different ways of making the reaction rate limited by the elongation. Since elongation of Aβ fibrils have a larger

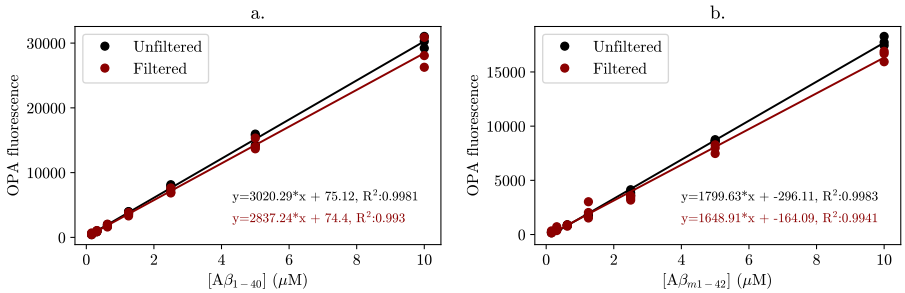

Figure 3.8: A serial dilution of Aβ1-40 (a.) or Aβ(M1-42) (b.) was done in DNA LoBind tubes (Eppendorf) and then either directly reacted with OPA (black circles) or first filtered through a GHP filter plate (red). Solid lines represent linear regressions fitted to all replicates (N=3) and weighted 1/C.

rate constant than the other processes but only happens at the fibril ends (in contrast to secondary nucleation that is catalyzed by the fibril surface), the signature of an elongation-dominated reaction is a linear increase in fibril mass. One way to make a reaction rate limited by elongation is thus to increase the number of ends relative to fibril mass. In paper III we did this by having a very high amount of seeds (50 %), which works but requires quite a lot of fibrils per sample. Therefore we investigated the effects of adding either sonicated or freeze-thawed fibrils. Both these processes leads to a breaking up of the fibrils into shorter fragments, thus increasing the number of fibril ends and potentially leading to an elongation-dominated reaction. As seen by the steeper initial slope in Figure 3.9, freeze-thawing is more effective at fragmenting the fibrils than a short sonication. Freeze-thawing also has the very practical benefit that you can prepare a lot of seeds at one point and freeze them for later use.

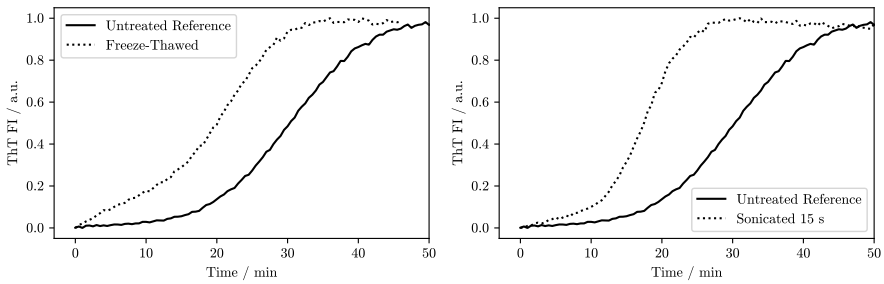

Figure 3.9: Normalized mean kinetic traces of Aβ(M1-42) seeded with untreated seeds (black), freeze-thawed seeds (dotted line left) or sonicated seeds (dotted line right). Sonication was done with a titanium exponential W/spanner 66C4 probe submerged in the sample with 1 s on, 1 s off and with an amplitude of 4.3 %. N=4

Chapter 4

Summary of Papers

I have during my PhD studies tried to add some fundamental insights into the kinetics and thermodynamics of amyloid formation, with the Aβ peptide as a model system. In order to facilitate the study of the thermodynamic driving forces behind amyloid formation, we started by developing a convenient and high-throughput method for solubility measurements. The temperature dependence of Aβ solubility was then investigated, in order to dissect the enthalpic and entropic contributions to the free energy difference, which determines the equilibrium between the phases composed of monomer in solution and solid fibrils. In parallel to this, a colleague of mine found that a fragment of the tau protein formed fibrils at widely different rates if incubated truly quiescent or under mild agitation, which lead us to an extensive investigation of the role of shear forces in amyloid formation. Finally, we have developed a simple kinetic assay to classify different morphs (or distributions of morphs) of amyloids based on their relative elongation rates at two different conditions.

4.1 Paper I: Solubility assay development

To better understand the role of solubility in the formation of amyloids I had the ambition to investigate many mutants under a lot of different conditions. Which quickly lead to the realization that this would mean hundreds, if not thousands, of samples. Therefore, we saw the need for a method that was quick, inexpensive and high-throughput. While there are such assays [24, 92, 93], some are not compatible with amyloids and some require labeling. We thus decided to develop a method that was optimal to study the solubility of amyloid forming peptides and proteins. To do this there were three main problems to overcome; adsorption, reaching equilibrium and quantifying only the monomers once equilibrium had been reached. Many different avenues were explored for each problem, such as low binding materials from different vendors, reaching equilibrium from different directions, centrifugation and filtration to separate out fibrils, concentrating the samples through lyophilizations, several different reactive fluorescent probes for quantification and amino acid analysis through acidic hydrolysis. The main conclusions of this effort is summarized in Chapter 3 of this thesis and it lead me to the development of the assay shown in Figure 4.1. In brief, the method works by setting up dilution series of the protein of interest in a way so that some solutions are so highly supersaturated that they will precipitate within an experimentally accessible time frame, while some samples are undersaturated and thus remain as one single phase with no aggregates. After a suitable incubation time, the formed aggregates can be removed by running all samples through a 96-well filter plate and the remaining soluble fraction can be quantified with OPA, giving a curve as in Figure 4.1:5. A standard curve can be constructed from the samples with concentrations ranging from the lowest initial concentrations to the highest which has not precipitated. Because of metastability, such a standard curve will cover a relevant concentration range for solubility. The protein concentration left in solution for the samples with precipitation can then be determined by the standard curve and represent the solubility of that protein under the conditions used.

To validate this assay we determined the solubility of Aβ40 at 37 °C in a buffer with 20 mM sodium phosphate, 0.2 mM EDTA, 0.02 % NaN_3, pH 7.4. These data were compared to solubility in the same buffer but after the addition of 150 mM NaCl, at a lower temperature (26 °C) and for a peptide variant with an extra methionine at the N-terminus, keeping all other conditions the same. The result can be seen in Figure 4.2.

In conclusion, Paper I introduces an inexpensive, high-troughput and label-free assay specialized for, but not limited to, amyloid proteins. With this assay we measure the solubility of Aβ40 under different conditions and compare the results to previously reported values.

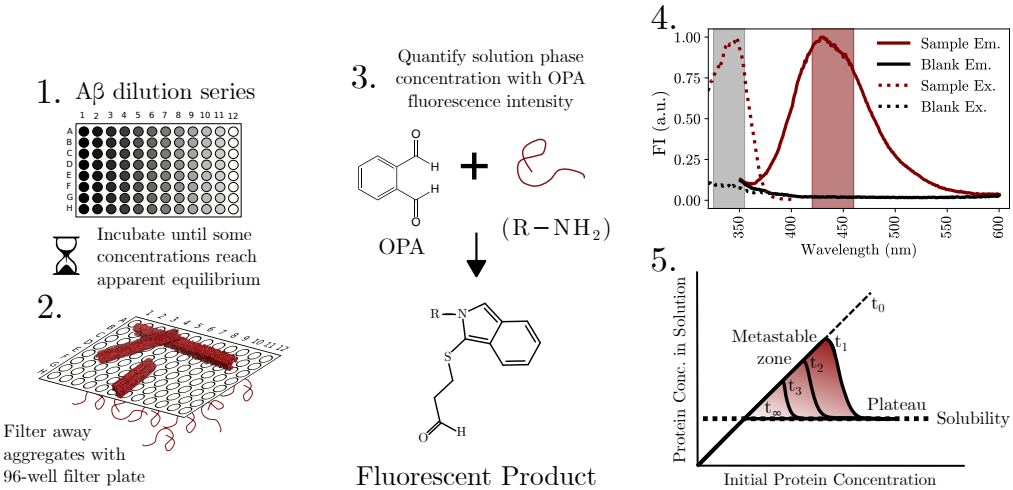

Figure 4.1: Overview of the developed solubility assay, adapted from Paper I [77] (CC-BY 4.0). 1. represent replicates of a concentration series of Aβ peptide in a PEG-ylated 96-well plate, 2. represent filtering away fibrils and other large aggregates from monomers using a 96-well filter plate (size of fibrils and monomers is obviously enlarged for pedagogic purposes), 3. shows a summary of the OPA reaction, 4. shows the spectroscopic result of the OPA reaction and 5. schematically illustrates a typical result of the assay.

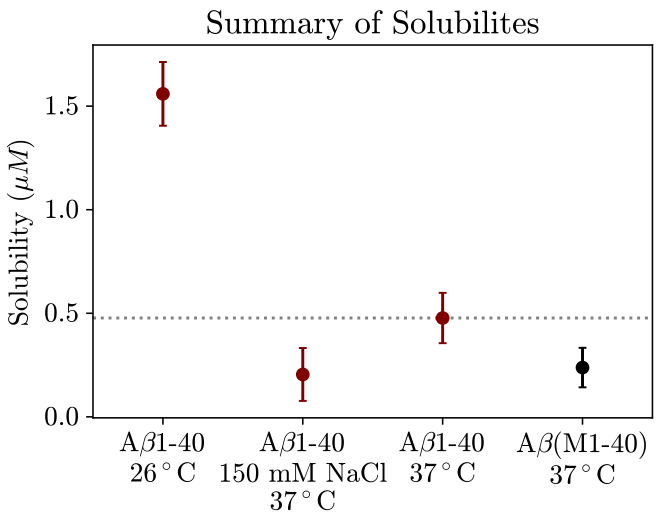

Figure 4.2: Summary of the solubilities established in Paper I, buffer conditions are, in addition to what is specified on the x-axis, 20 mM sodium phosphate, 0.2 mM EDTA, 0.02 % NaN_3, pH 7.4. Figure reproduced from Paper I [77] (CC-BY 4.0).

4.2 Paper II: Temperature Dependence of Aβ Solubility

Temperature dependent data may reveal the driving forces behind protein folding [94], which here motivated the investigations of the solubility of the Aβ peptide over a range of different temperatures. To achieve this, we incubated Aβ42 (in low binding tubes), at temperatures ranging from 10 to 80 °C. After incubation, the test tubes were put on ice to minimize further elongation [91] and centrifuged to pellet fibrils. The monomer concentration in the supernatant were then quantified with HPLC-MS. This revealed a non-monotonic temperature dependence of the solubility, with the temperature of lowest solubility (T_{min}), found approximately at body temperature, Figure 4.3. These results were corroborated with circular dichroism (CD) spectra showing β-sheet signal oppositely aligned to the solubility trend. The results are also in line with earlier reports for other amyloid systems, including α-synuclein [95] and β2-microglobulin [96]. The experimental data in Figure 4.3 can be fitted to a thermodynamic model based on Eq. 2.1, describing the equilibrium between monomer in solution and the solid fibril phase. With the isobaric definition of heat capacity ($\Delta C_p = d\Delta h^\circ/dT$) we obtain an expression of the temperature dependence of $\Delta\mu^\circ(T)$ (Eq. 4.1), where T_h and T_s correspond to the temperatures where $\Delta h = 0$ and $\Delta s = 0$, respectively (for more details, see Paper II). Based on this, we can calculate the partial molar enthalpic and entropic contributions for determining the equilibrium between monomers and fibrils at the different temperatures, Figure 4.4.

$$\Delta\mu^\circ(T) = \Delta C_p[(T - T_h) - T\ln(T/T_s)] \tag{4.1}$$

The fit shows that enthalpy opposes and entropy favors amyloid formation at temperatures below T_{min} and vice versa at higher temperatures. These findings are in alignment with both experimental data [97–99] and simulations [100, 101] of other amyloid systems.

In conclusion, Paper II provides experimental evidence that the solubility of the Aβ peptide show similar non-monotonic temperature dependence as the folding-unfolding equilibrium of most proteins [94]. The data strongly suggest that uni-molecular and multi-molecular protein folding share the same driving force, which for both cases is likely to be governed by the hydrophobic effect [7, 94, 99–101].

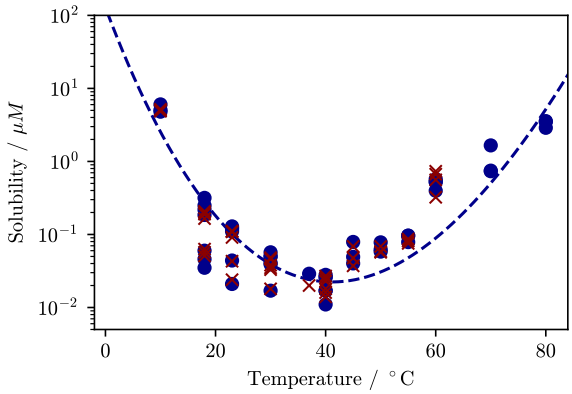

Figure 4.3: Temperature dependence of Aβ42 solubility plotted with a logarithmic scale. Blue circles are measurements by MS and red crosses are measurements by UV absorbance at 205 nm. Equation 4.1 and 2.1 are fitted to the mean of 1-3 replicates at each temperature and incubation time (dashed line). The parameter values obtained for this fit are: $\Delta C_p = 6.94 \pm 0.5$ kJ/mol, $T_h = 314.21 \pm 0.81$ K and $T_s = 315.64 \pm 0.85$ K.

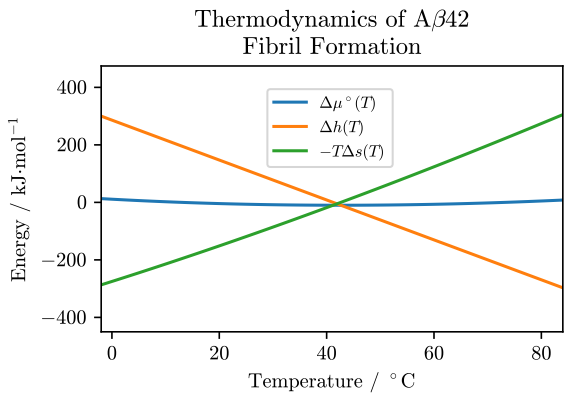

Figure 4.4: Temperature dependence of the difference in chemical potential between monomers in solution and monomers in fibrils (blue), as calculated by Eq. 4.1, and it's partial molar components as calculated by $\Delta h^\circ(T) = \Delta C_p(T - T_h)$ (orange) and $\Delta s^\circ(T) = \Delta C_p \ln(T/T_s)$ (green) [9].

4.3 Paper III: The Effect of Gentle Agitation

This study started with an observation made by a colleague of mine, that the gentle agitation introduced by just measuring samples in a plate reader accelerated the amyloid formation kinetics manyfold. The same effect had been observed earlier by another group for the IAPP peptide [22]. Based on these observations, we raised the question if this could be a general phenomenon in amyloid formation. We therefore performed analogous experiments also for Aβ40 and Aβ42, again observing the same effects of gentle agitation. Data for 4 different proteins are summarized in Figure 4.6.

We next aimed for mechanistic understanding of these effects and decided to go into more detailed studies for one of the peptides, Aβ42. Initially we questioned that the effects of mild agitation are due to fragmentation of fibrils, which is the reported consequence of more vigorous shaking [25]. A first step to get mechanistic insights of amyloid formation is to plot the logarithm of the half-time (the time it takes the reaction to reach 50 % fibril mass) against the logarithm of the initial monomer concentration. If the reaction is rate limited by fragmentation, such a log-log plot will scale linearly with a slope of -0.5 [102]. What we found for reactions with this gentle agitation though, was a slope of -1.44. We could then conclude that fragmentation was not rate limiting under these conditions and thus, any effect that gentle agitation might have on the fragmentation of fibrils is not enough to explain the overall speed up.

Our second hypothesis was that secondary nucleation was affected by the gentle agitation. To test this we inhibited most, if not all, secondary nucleation by adding the brichos domain from proSP-C, which has previously been shown to effectively inhibit secondary nucleation [103]. Interestingly, the effect caused by the mild agitation did not only remain, but actually increased under these conditions. This lead us to the conclusion that the gentle agitation must affect the primary nucleation and/or the elongation of fibrils.

Since we knew that fragmentation was negligible under these conditions and that almost all secondary nucleation was inhibited because of the presence of brichos, we could calculate that the effect on the product of the rate constants for elongation (k_+) and primary nucleation (k_n), k_+k_n, which was shown to differ by a factor of 12 between continuous reading and reading every 15 minutes. If the effect of gentle agitation was because of an increase in elongation rate, the fibrils would be longer, on average, in samples that were read continuously. Whether this is the case can be investigated by highly seeded reactions, using seeds that have been produced with or without the gentle agitation. Longer fibrils would then give a lower reaction rate. During our investigation we found that seeds formed under agitation gave an accelerated reaction rate and thus contain, on average, shorter fibrils. From this result, we can conclude that it is the primary nucleation rate constant that is responsible for the change in k_+k_n. However, global fitting to concentration-dependent

kinetics monitored with or without the agitation could not properly explain the data, unless the secondary nucleation rate constant k_2 was also altered by a factor of 4. In conclusion, effects on both primary and secondary nucleation are responsible for the acceleration of fibril formation caused by gentle agitation, Figure 4.5.

To further strengthen this conclusion, we performed cryo-EM and microfluidic free-flow electrophoresis (μFFE). The cryo-TEM images showed that decorations on the fibrils, believed to be related to secondary nucleation [104], disappear upon vortexing. This tells us that relatively low shear forces are sufficient to rip off these structures but not enough for any clearly visible fragmentation. From the μFFE experiment, we could estimate the number of oligomers at the half-time of the fibril formation reaction. These experments found that more oligomers are present in the sample that had been prepared under gentle agitation, in line with the two nucleation processes being accelerated.

In conclusion we determined the mechanistic reasons for why Aβ(M1-42) forms fibrils quicker when under gentle agitation compared to fully quiescent conditions. Through a combination of experiments using different conditions and techniques, we propose that shear forces facilitate the removal of nuclei from surfaces which accelerates both primary and secondary nucleation, while elongation and fragmentation is affected in negligible amounts. This contributes to the fundamental understanding of amyloid formation mechanisms and could facilitate pharmaceutical drug screening. It could also serve as a means to gain further control of kinetic assays and a certain degree of shear forces might actually resemble the situation *in vivo* [105, 106].

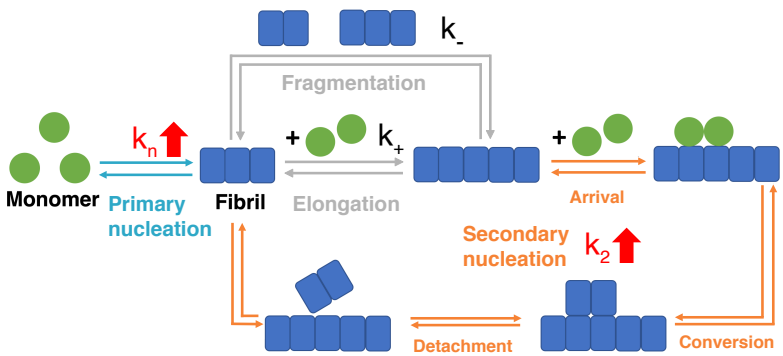

Figure 4.5: Summary of the effect on Aβ(M1-42) aggregation kinetics by gentle agitation. Figure is reproduced unaltered from Axell et al. [41] and is under a CC BY-NC-ND 4.0 license.

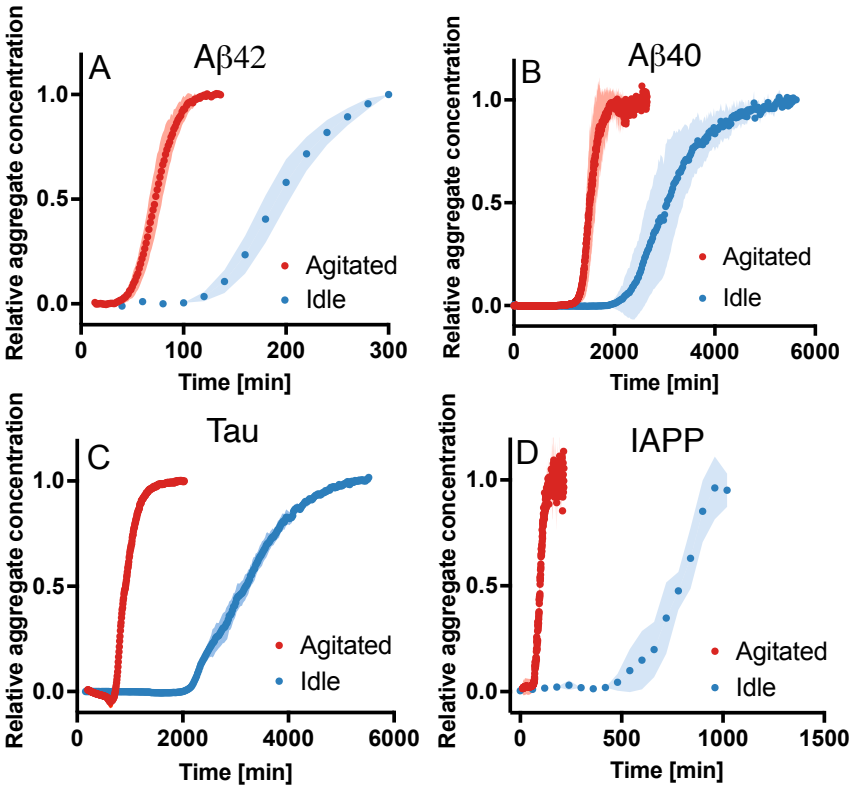

Figure 4.6: Aggregation kinetics for four amyloid systems where the reaction is performed either with continuous (agitated, red) or infrequent (idle, blue) reading. Data for IAPP is from Sebastiao et al. [22]. Markers represent the mean values of 8, 4, 3 and 3 replicates for A, B, C and D, respectively. Shaded areas represent standard deviation. Figure is reproduced unaltered from Axell et al. [41] and is under a CC BY-NC-ND 4.0 license.

4.4 Paper IV: Differentiating Amyloid Morphs

This manuscript is motivated by the apparent polymorphism of amyloid fibrils and its relevance for disease [107]. While the particular structure of an amyloid fibril is usually referred to as a "polymorph" (including filament fold, filament assembly, fibril twist etc.) [40], we here instead choose to use the term "morph", as "poly" means several [108]. The assumption behind this manuscript is that different morphs should have different properties, thus morphs could be classified based on their properties. The property we primarily look at in this paper is the temperature dependence of the elongation rate constant, k_+. To evaluate this property of different fibrils, we break them apart by freeze-thawing and sonication as detailed in section 3.5. Thus we enter an elongation-dominated regime of the aggregation process, and the slope of fibril mass vs time corresponds to $2k_+P_0[m]$, where P_0 is the number of fibrils and $[m]$ is the monomer concentration [53]. If aggregation kinetics is performed at two separate temperatures with seeds from the same aliquot and with the same monomer concentration, the change in k_+ due to temperature is given by the ratio of the slopes.

As an initial test case for this assay we prepared fibrils at several temperatures between 10 and 70 °C, which turned out to produce different morph distributions according to cryo-EM (but with similar filament fold). We then tested these fibril samples in the assay, using fibrils prepared at different temperatures as seeds. The result can be found in Figure 4.7, displaying selected kinetic traces with the intial slopes marked in orange, and the ratio of initial slope at high and low measurement temperatures for fibrils formed at temperatures 10 to 70 °C as a bar chart. The resulting ratios, and thus temperature dependence of elongation rate constant, for all fibrils formed at 10 to 50 °C are similar and are therefore classified as the same morph with respect to their seeding capacity, while the fibrils formed at 60 and 70 °C stand out and are thus classified as being different morphs. This classification is corroborated by the differences in ThT intensity per fibril mass.

We aim at an assay that can elucidate how the structural elements of different fibril morphs affect their fibril seeding properties. The assay could also find applications in quality controls of fibrillar samples, e.g. to verify the same morph (or morph distribution) is present at the start of each experiment. On longer terms, this assay may also be used in diagnostics in cases where the assayed property correlates strongly to with disease pathology.

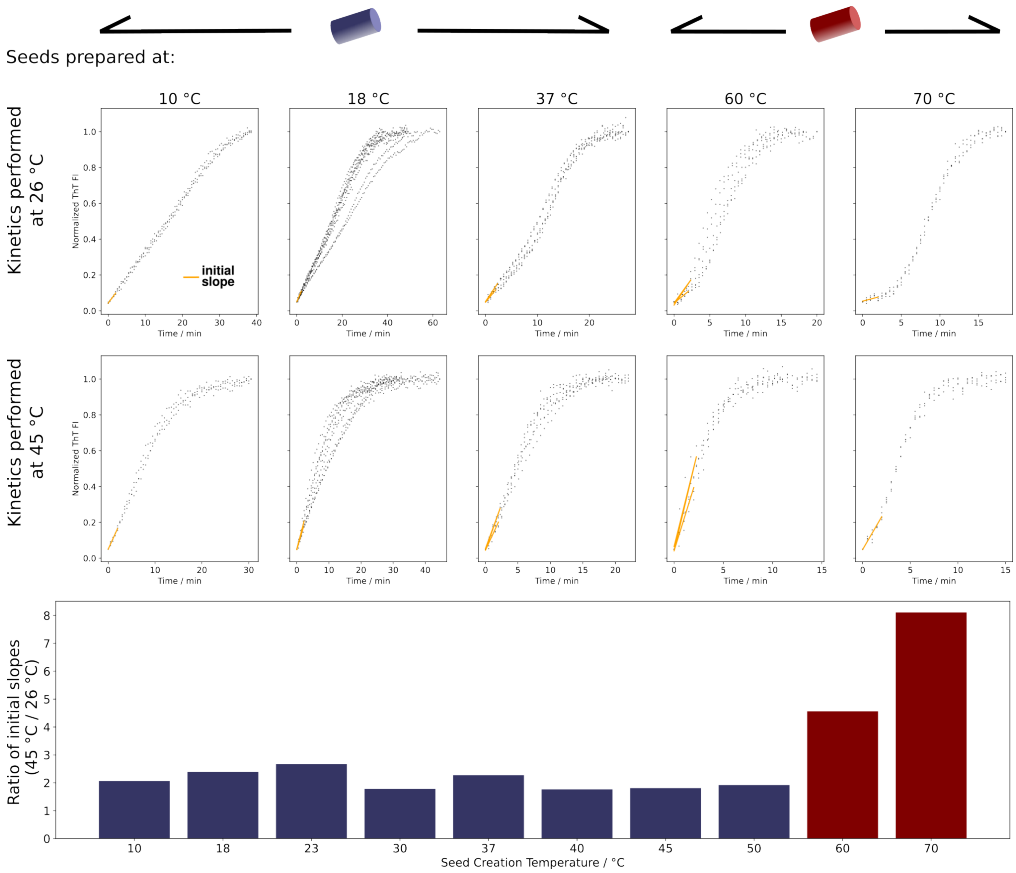

Figure 4.7: Representative kinetic traces measured at either 26 °C (top row) or 45 °C (middle row) and the ratios of initial slopes (bottom row). The slopes are linear regressions fitted to the first 2.5 minutes of all replicates per experiment, the presence of multiple intial slopes in a single graph is thus because that seed was assayed more than once in separate experiments. Ratios are the slope at 45 °C divided by the slope at 26 °C. The different strains are color coded as blue (left) and red (right).

Chapter 5

Concluding remarks

This thesis presents two developed assays, an investigation of the temperature dependence of Aβ solubility and a mechanistic study of how gentle agitation affect fibril formation kinetic. Thus, the thesis provides a tool to facilitate solubility studies of amyloid proteins in a label-free and high-throughput manner (Paper I). It contributes to the understanding of the thermodynamic driving forces behind Aβ aggregation (Paper II). Through a combination of kinetic experiments, ultrastructural studies and single-molecule measurements, the effect of gentle agitation on primary and secondary nucleation in Aβ42 fibril formation are quantified and mechanistically explained (Paper III). Finally, an assay to differentiate morphs (or distributions of morphs) based on their relative elongation rates at different conditions is presented, which shows that fibrils formed at 60 and 70 °C are markedly different in this aspect than fibrils formed at temperatures from 10 to 50 °C (Paper IV).

If I had more time I would like to further investigate the following outstanding questions:

1. How does the amino acid sequence of a intrinsically disordered protein govern it's solubility?
2. How does the solution conditions affect the solubility of a given protein? And why?
3. How similar is the effect of gentle agitation on the microscopic processes in different amyloid systems?
4. What structural elements of amyloid fibrils affect the activation energy of fibril elongation and how?

Bibliography

1. Vickery, H. B. The Origin of the Word Protein. *The Yale Journal of Biology and Medicine* **22,** 387–393. pmid: 15413335 (May 1950).
2. Hartley, H. Origin of the Word 'Protein'. *Nature* **168,** 244–244. doi:10.1038/168244a0 (4267 Aug. 1951).
3. Huddy, T. F. *et al.* Blueprinting Extendable Nanomaterials with Standardized Protein Blocks. *Nature* **627,** 898–904. doi:10.1038/s41586-024-07188-4 (Mar. 2024).
4. Koh, L.-D. *et al.* Structures, Mechanical Properties and Applications of Silk Fibroin Materials. *Progress in Polymer Science* **46,** 86–110. doi:10.1016/j.progpolymsci.2015.02.001 (July 1, 2015).
5. Dobson, C. M. Protein Folding and Misfolding. *Nature* **426,** 884–890. doi:10.1038/nature02261 (Dec. 2003).
6. Oldfield, C. J. & Dunker, A. K. Intrinsically Disordered Proteins and Intrinsically Disordered Protein Regions. *Annual Review of Biochemistry* **83,** 553–584. doi:10.1146/annurev-biochem-072711-164947 (June 2, 2014).
7. Tanford, C. How Protein Chemists Learned about the Hydrophobic Factor. *Protein Science* **6,** 1358–1366. doi:10.1002/pro.5560060627 (1997).
8. Atkins, P. W. & De Paula, J. *Physical Chemistry for the Life Sciences* 2nd ed (W.H. Freeman and Co. ; Oxford University Press, New York, Oxford, 2011).
9. Southall, N. T., Dill, K. A. & Haymet, A. D. J. A View of the Hydrophobic Effect. *The Journal of Physical Chemistry B* **106,** 521–533. doi:10.1021/jp015514e (Jan. 1, 2002).
10. Schauperl, M., Podewitz, M., Waldner, B. J. & Liedl, K. R. Enthalpic and Entropic Contributions to Hydrophobicity. *Journal of Chemical Theory and Computation* **12,** 4600–4610. doi:10.1021/acs.jctc.6b00422 (9 Sept. 13, 2016).
11. Hopp, T. P. & Woods, K. R. Prediction of Protein Antigenic Determinants from Amino Acid Sequences. *Proceedings of the National Academy of Sciences* **78,** 3824–3828. doi:10.1073/pnas.78.6.3824 (June 1981).

12. Janin, J. Surface and inside Volumes in Globular Proteins. *Nature* **277**, 491–492. doi:10.1038/277491a0 (Feb. 1979).

13. Engelman, D. M., Steitz, T. A. & Goldman, A. IDENTIFYING NONPOLAR TRANSBILAYER HELICES IN AMINO ACID SEQUENCES OF MEMBRANE PROTEINS. *Annual Review of Biophysics* **15**, 321–353. doi:10.1146/annurev.bb.15.060186.001541 (Volume 15, 1986 June 9, 1986).

14. Kyte, J. & Doolittle, R. F. A Simple Method for Displaying the Hydropathic Character of a Protein. *Journal of Molecular Biology* **157**, 105–132. doi:10.1016/0022-2836(82)90515-0 (May 5, 1982).

15. Eisenberg, D., Schwarz, E., Komaromy, M. & Wall, R. Analysis of Membrane and Surface Protein Sequences with the Hydrophobic Moment Plot. *Journal of Molecular Biology* **179**, 125–142. doi:10.1016/0022-2836(84)90309-7 (Oct. 15, 1984).

16. Cornette, J. L. *et al.* Hydrophobicity Scales and Computational Techniques for Detecting Amphipathic Structures in Proteins. *Journal of Molecular Biology* **195**, 659–685. doi:10.1016/0022-2836(87)90189-6 (June 5, 1987).

17. Buxbaum, J. N. *et al.* Amyloid Nomenclature 2024: Update, Novel Proteins, and Recommendations by the International Society of Amyloidosis (ISA) Nomenclature Committee. *Amyloid* **0**, 1–8. doi:10.1080/13506129.2024.2405948. pmid: 39350582 (2024).

18. Kyle, R. A. Amyloidosis: A Convoluted Story. *British Journal of Haematology* **114**, 529–538. doi:10.1046/j.1365-2141.2001.02999.x (2001).

19. Tagarelli, A., Piro, A., Tagarelli, G., Lagonia, P. & Quattrone, A. Alois Alzheimer: A Hundred Years after the Discovery of the Eponymous Disorder. *International Journal of Biomedical Science : IJBS* **2**, 196–204. pmid: 23674983 (June 2006).

20. Glenner, G. G. & Wong, C. W. Alzheimer's Disease: Initial Report of the Purification and Characterization of a Novel Cerebrovascular Amyloid Protein. *Biochemical and Biophysical Research Communications* **120**, 885–890. doi:10.1016/S0006-291X(84)80190-4 (3 May 16, 1984).

21. Hortschansky, P., Schroeckh, V., Christopeit, T., Zandomeneghi, G. & Fändrich, M. The Aggregation Kinetics of Alzheimer's β-Amyloid Peptide Is Controlled by Stochastic Nucleation. *Protein Science : A Publication of the Protein Society* **14**, 1753–1759. doi:10.1110/ps.041266605. pmid: 15937275 (July 2005).

22. Sebastiao, M., Quittot, N. & Bourgault, S. Thioflavin T Fluorescence to Analyse Amyloid Formation Kinetics: Measurement Frequency as a Factor Explaining Irreproducibility. *Analytical Biochemistry* **532**, 83–86. doi:10.1016/j.ab.2017.06.007 (Sept. 1, 2017).

23. Zagorski, M. G. *et al.* in *Methods in Enzymology* 189–204 (Academic Press, Jan. 1, 1999). doi:10.1016/S0076-6879(99)09015-1.

24. Hellstrand, E., Boland, B., Walsh, D. M. & Linse, S. Amyloid β-Protein Aggregation Produces Highly Reproducible Kinetic Data and Occurs by a Two-Phase Process. *ACS Chemical Neuroscience* **1**, 13–18. doi:10.1021/cn900015v (Jan. 20, 2010).

25. Cohen, S. I. A. *et al.* Proliferation of Amyloidβ-42 Aggregates Occurs through a Secondary Nucleation Mechanism. *Proceedings of the National Academy of Sciences of the United States of America* **110**, 9758–9763. doi:10.1073/pnas.1218402110. pmid: 23703910 (24 June 11, 2013).

26. Buell, A. Stability Matters, Too - The Thermodynamics of Amyloid Fibril Formation. *Chemical Science.* doi:10.1039/D1SC06782F (Feb. 2, 2022).

27. *The Nobel Prize in Chemistry 2017* NobelPrize.org. https://www.nobelprize.org/prizes/chemistry/2017/popular-information/ (2024).

28. Fitzpatrick, A. W. P. *et al.* Cryo-EM Structures of Tau Filaments from Alzheimer's Disease. *Nature* **547**, 185–190. doi:10.1038/nature23002 (7662 July 2017).

29. Gremer, L. *et al.* Fibril Structure of Amyloid-β(1–42) by Cryo–Electron Microscopy. *Science* **358**, 116–119. doi:10.1126/science.aao2825 (6359 Oct. 6, 2017).

30. Colvin, M. T. *et al.* Atomic Resolution Structure of Monomorphic Aβ42 Amyloid Fibrils. *Journal of the American Chemical Society* **138**, 9663–9674. doi:10.1021/jacs.6b05129 (Aug. 3, 2016).

31. Smaoui, M. R. *et al.* Computational Assembly of Polymorphic Amyloid Fibrils Reveals Stable Aggregates. *Biophysical Journal* **104**, 683–693. doi:10.1016/j.bpj.2012.12.037 (Feb. 5, 2013).

32. Schrödinger, LLC. *The PyMOL Molecular Graphics System, Version 1.8* Nov. 2015.

33. Scheres, S. H., Zhang, W., Falcon, B. & Goedert, M. Cryo-EM Structures of Tau Filaments. *Current Opinion in Structural Biology* **64**, 17–25. doi:10.1016/j.sbi.2020.05.011 (Oct. 2020).

34. Jarrett, J. T., Berger, E. P. & Lansbury, P. T. The Carboxy Terminus of the .Beta. Amyloid Protein Is Critical for the Seeding of Amyloid Formation: Implications for the Pathogenesis of Alzheimer's Disease. *Biochemistry* **32**, 4693–4697. doi:10.1021/bi00069a001 (18 May 11, 1993).

35. Michaels, T. C. T. *et al.* Amyloid Formation as a Protein Phase Transition. *Nature Reviews Physics* **5**, 379–397. doi:10.1038/s42254-023-00598-9 (June 27, 2023).

36. Pálmadóttir, T. *et al.* Morphology-Dependent Interactions between α-Synuclein Monomers and Fibrils. *International Journal of Molecular Sciences* **24**, 5191. doi:10.3390/ijms24065191 (6 Jan. 2023).

37. Padrick, S. B. & Miranker, A. D. Islet Amyloid: Phase Partitioning and Secondary Nucleation Are Central to the Mechanism of Fibrillogenesis. *Biochemistry* **41,** 4694–4703. doi:10.1021/bi0160462. pmid: 11926832 (Apr. 9, 2002).

38. Tanaka, M., Collins, S. R., Toyama, B. H. & Weissman, J. S. The Physical Basis of How Prion Conformations Determine Strain Phenotypes. *Nature* **442,** 585–589. doi:10.1038/nature04922 (Aug. 2006).

39. Ruschak, A. M. & Miranker, A. D. Fiber-Dependent Amyloid Formation as Catalysis of an Existing Reaction Pathway. *Proceedings of the National Academy of Sciences of the United States of America* **104,** 12341–12346. doi:10.1073/pnas.0703306104. pmid: 17640888 (July 24, 2007).

40. Ke, P. C. *et al.* Half a Century of Amyloids: Past, Present and Future. *Chemical Society Reviews* **49,** 5473–5509. doi:10.1039/C9CS00199A (Aug. 3, 2020).

41. Axell, E. *et al.* The Role of Shear Forces in Primary and Secondary Nucleation of Amyloid Fibrils. *Proceedings of the National Academy of Sciences* **121,** e2322572121. doi:10.1073/pnas.2322572121 (June 18, 2024).

42. Knowles, T. P. J. *et al.* An Analytical Solution to the Kinetics of Breakable Filament Assembly. *Science* **326,** 1533–1537. doi:10.1126/science.1178250 (Dec. 11, 2009).

43. Oosawa, F. & Kasai, M. A Theory of Linear and Helical Aggregations of Macromolecules. *Journal of Molecular Biology* **4,** 10–21. doi:10.1016/S0022-2836(62)80112-0 (Jan. 1962).

44. Pallitto, M. M. & Murphy, R. M. A Mathematical Model of the Kinetics of Beta-Amyloid Fibril Growth from the Denatured State. *Biophysical Journal* **81,** 1805–1822. pmid: 11509390 (3 Sept. 2001).

45. Gade Malmos, K. *et al.* ThT 101: A Primer on the Use of Thioflavin T to Investigate Amyloid Formation. *Amyloid* **24,** 1–16. doi:10.1080/13506129.2017.1304905 (Jan. 2, 2017).

46. Cohen, S. I. A. *et al.* Nucleated Polymerization with Secondary Pathways. I. Time Evolution of the Principal Moments. *The Journal of Chemical Physics* **135,** 065105. doi:10.1063/1.3608916 (Aug. 12, 2011).

47. Cohen, S. I. A., Vendruscolo, M., Dobson, C. M. & Knowles, T. P. J. Nucleated Polymerization with Secondary Pathways. II. Determination of Self-Consistent Solutions to Growth Processes Described by Non-Linear Master Equations. *The Journal of Chemical Physics* **135,** 065106. doi:10.1063/1.3608917 (Aug. 12, 2011).

48. Meisl, G. *et al.* Molecular Mechanisms of Protein Aggregation from Global Fitting of Kinetic Models. *Nature Protocols* **11,** 252–272. doi:10.1038/nprot.2016.010 (2 Feb. 2016).

49. Michaels, T. C. T., Cohen, S. I. A., Vendruscolo, M., Dobson, C. M. & Knowles, T. P. J. Hamiltonian Dynamics of Protein Filament Formation. *Physical Review Letters* **116,** 038101. doi:10.1103/PhysRevLett.116.038101 (Jan. 22, 2016).

50. Dear, A. J. *et al.* The Catalytic Nature of Protein Aggregation. *The Journal of Chemical Physics* **152,** 045101. doi:10.1063/1.5133635 (Jan. 28, 2020).

51. Linse, S. *et al.* Kinetic Fingerprints Differentiate the Mechanisms of Action of Anti-Aβ Antibodies. *Nature Structural & Molecular Biology.* doi:10.1038/s41594-020-0505-6. pmid: 32989305 (Sept. 28, 2020).

52. *Aducanumab to Be Discontinued as an Alzheimer's Treatment* Alzheimer's Disease and Dementia. https://alz.org/alzheimers-dementia/treatments/aducanumab (2024).

53. Arosio, P., Knowles, T. P. J. & Linse, S. On the Lag Phase in Amyloid Fibril Formation. *Physical Chemistry Chemical Physics* **17,** 7606–7618. doi:10.1039/C4CP05563B (12 Mar. 11, 2015).

54. Munke, A. *et al.* Phage Display and Kinetic Selection of Antibodies That Specifically Inhibit Amyloid Self-Replication. *Proceedings of the National Academy of Sciences* **114,** 6444–6449. doi:10.1073/pnas.1700407114 (June 20, 2017).

55. Housmans, J. A. J., Wu, G., Schymkowitz, J. & Rousseau, F. A Guide to Studying Protein Aggregation. *The FEBS Journal* **290,** 554–583. doi:10.1111/febs.16312 (Feb. 2023).

56. Naiki, H., Higuchi, K., Hosokawa, M. & Takeda, T. Fluorometric Determination of Amyloid Fibrils *in Vitro* Using the Fluorescent Dye, Thioflavine T. *Analytical Biochemistry* **177,** 244–249. doi:10.1016/0003-2697(89)90046-8 (Mar. 1, 1989).

57. Xue, C., Lin, T. Y., Chang, D. & Guo, Z. Thioflavin T as an Amyloid Dye: Fibril Quantification, Optimal Concentration and Effect on Aggregation. *Royal Society Open Science* **4,** 160696. doi:10.1098/rsos.160696.

58. Ziaunys, M., Sneideris, T. & Smirnovas, V. Formation of Distinct Prion Protein Amyloid Fibrils under Identical Experimental Conditions. *Scientific Reports* **10,** 4572. doi:10.1038/s41598-020-61663-2 (Mar. 12, 2020).

59. LeVine, H. Thioflavine T Interaction with Synthetic Alzheimer's Disease Beta-Amyloid Peptides: Detection of Amyloid Aggregation in Solution. *Protein Science : A Publication of the Protein Society* **2,** 404–410. pmid: 8453378 (3 Mar. 1993).

60. *The Nobel Prize in Chemistry 2024* NobelPrize.org. https://www.nobelprize.org/prizes/chemistry/2024/press-release/ (2024).

61. Jumper, J. *et al.* Highly Accurate Protein Structure Prediction with AlphaFold. *Nature* **596,** 583–589. doi:10.1038/s41586-021-03819-2 (Aug. 2021).

62. Ragonis-Bachar, P. *et al.* What Can AlphaFold Do for Antimicrobial Amyloids? *Proteins: Structure, Function, and Bioinformatics* **92,** 265–281. doi:10.1002/prot.26618 (2024).

63. Cherny, I. & Gazit, E. Amyloids: Not Only Pathological Agents but Also Ordered Nanomaterials. *Angewandte Chemie International Edition* **47,** 4062–4069. doi:10.1002/anie.200703133 (22 2008).

64. Wei, G. *et al.* Self-Assembling Peptide and Protein Amyloids: From Structure to Tailored Function in Nanotechnology. *Chemical Society Reviews* **46,** 4661–4708. doi:10.1039/C6CS00542J (July 31, 2017).

65. Li, C., Qin, R., Liu, R., Miao, S. & Yang, P. Functional Amyloid Materials at Surfaces/Interfaces. *Biomaterials Science* **6,** 462–472. doi:10.1039/C7BM01124E (3 Feb. 27, 2018).

66. Scheibel, T. *et al.* Conducting Nanowires Built by Controlled Self-Assembly of Amyloid Fibers and Selective Metal Deposition. *Proceedings of the National Academy of Sciences* **100,** 4527–4532. doi:10.1073/pnas.0431081100 (Apr. 15, 2003).

67. Kamada, A. *et al.* Controlled Self-Assembly of Plant Proteins into High-Performance Multifunctional Nanostructured Films. *Nature Communications* **12,** 3529. doi:10.1038/s41467-021-23813-6 (June 10, 2021).

68. Diaz, C. & Missirlis, D. Amyloid-Based Albumin Hydrogels. *Advanced Healthcare Materials* **n/a,** 2201748. doi:10.1002/adhm.202201748 (n/a Feb. 16, 2023).

69. Su, J. *et al.* Single-Site Iron-Anchored Amyloid Hydrogels as Catalytic Platforms for Alcohol Detoxification. *Nature Nanotechnology* **19,** 1168–1177. doi:10.1038/s41565-024-01657-7 (Aug. 2024).

70. Shen, L., Adachi, T., Vanden Bout, D. & Zhu, X.-Y. A Mobile Precursor Determines Amyloid-β Peptide Fibril Formation at Interfaces. *Journal of the American Chemical Society* **134,** 14172–14178. doi:10.1021/ja305398f (34 Aug. 29, 2012).

71. Linse, S. in *Intrinsically Disordered Proteins: Methods and Protocols* (eds Kragelund, B. B. & Skriver, K.) 731–754 (Springer US, New York, NY, 2020). doi:10.1007/978-1-0716-0524-0_38.

72. Anthis, N. J. & Clore, G. M. Sequence-Specific Determination of Protein and Peptide Concentrations by Absorbance at 205 Nm. *Protein Science : A Publication of the Protein Society* **22,** 851–858. doi:10.1002/pro.2253. pmid: 23526461 (June 2013).

73. Snyder, L. R., Kirkland, J. J. & Dolan, J. W. *Introduction to Modern Liquid Chromatography* 3rd ed. 912 pp. (Wiley, Hoboken, N.J, 2010).

74. Roth, Marc. Fluorescence Reaction for Amino Acids. *Analytical Chemistry* **43,** 880–882. doi:10.1021/ac60302a020 (7 June 1, 1971).

75. Benson, J. R. & Hare, P. E. O-Phthalaldehyde: Fluorogenic Detection of Primary Amines in the Picomole Range. Comparison with Fluorescamine and Ninhydrin. *Proceedings of the National Academy of Sciences* **72**, 619–622. doi:10.1073/pnas.72.2.619 (Feb. 1, 1975).

76. Simons, S. S. J. & Johnson, D. F. Reaction of O-Phthalaldehyde and Thiols with Primary Amines: Formation of 1-Alkyl(and Aryl)Thio-2-Alkylisoindoles. *The Journal of Organic Chemistry* **43**, 2886–2891. doi:10.1021/jo00408a030 (July 1, 1978).

77. Lindberg, M., Axell, E., Sparr, E. & Linse, S. A Label-Free High-Throughput Protein Solubility Assay and Its Application to Aβ40. *Biophysical Chemistry* **307**, 107165. doi:10.1016/j.bpc.2023.107165 (Apr. 1, 2024).

78. Lattanzi, V., Bernfur, K., Sparr, E., Olsson, U. & Linse, S. Solubility of Aβ40 Peptide. *JCIS Open* **4**, 100024. doi:10.1016/j.jciso.2021.100024 (Dec. 1, 2021).

79. Auer, S. Nucleation of Polymorphic Amyloid Fibrils. *Biophysical Journal* **108**, 1176–1186. doi:10.1016/j.bpj.2015.01.013 (Mar. 10, 2015).

80. Reynolds, N. P. *et al.* Competition between Crystal and Fibril Formation in Molecular Mutations of Amyloidogenic Peptides. *Nature Communications* **8**, 1338. doi:10.1038/s41467-017-01424-4 (1 Nov. 7, 2017).

81. Goto, Y., Noji, M., Nakajima, K. & Yamaguchi, K. Supersaturation-Dependent Formation of Amyloid Fibrils. *Molecules* **27**, 4588. doi:10.3390/molecules27144588 (14 Jan. 2022).

82. Sengupta, P. *et al.* The Amyloid β Peptide (Aβ1-40) Is Thermodynamically Soluble at Physiological Concentrations. *Biochemistry* **42**, 10506–10513. doi:10.1021/bi0341410 (35 Sept. 1, 2003).

83. Mok, Y.-F. & Howlett, G. J. in *Methods in Enzymology* 199–217 (Elsevier, 2006). doi:10.1016/S0076-6879(06)13011-6.

84. O'Nuallain, B. *et al.* in *Methods in Enzymology* 34–74 (Elsevier, 2006). doi:10.1016/S0076-6879(06)13003-7.

85. Bruggink, K. A., Müller, M., Kuiperij, H. B. & Verbeek, M. M. Methods for Analysis of Amyloid-β Aggregates. *Journal of Alzheimer's Disease* **28**, 735–758. doi:10.3233/JAD-2011-111421 (Feb. 20, 2012).

86. Stern, A. M. *et al.* Abundant Aβ Fibrils in Ultracentrifugal Supernatants of Aqueous Extracts from Alzheimer's Disease Brains. *Neuron.* doi:10.1016/j.neuron.2023.04.007 (May 10, 2023).

87. Arosio, P., Cedervall, T., Knowles, T. P. & Linse, S. Analysis of the Length Distribution of Amyloid Fibrils by Centrifugal Sedimentation. *Analytical Biochemistry* **504**, 7–13. doi:10.1016/j.ab.2016.03.015 (July 2016).

88. Beckman. *Using K-Factor to Compare Rotor Efficiency* https://www.beckman.com/resources/reading-material/application-notes/using-k-factor-to-compare-rotor-efficiency (2024).

89. Nasir, I., Linse, S. & Cabaleiro-Lago, C. Fluorescent Filter-Trap Assay for Amyloid Fibril Formation Kinetics in Complex Solutions. *ACS Chemical Neuroscience* **6,** 1436–1444. doi:10.1021/acschemneuro.5b00104. pmid: 25946560 (8 May 6, 2015).

90. Arosio, P., Cukalevski, R., Frohm, B., Knowles, T. P. J. & Linse, S. Quantification of the Concentration of Aβ42 Propagons during the Lag Phase by an Amyloid Chain Reaction Assay. *Journal of the American Chemical Society* **136,** 219–225. doi:10.1021/ja408765u (Jan. 8, 2014).

91. Cohen, S. I. A. *et al.* Distinct Thermodynamic Signature of Oligomer Generation in the Aggregation of the Amyloid-β Peptide. *Nature chemistry* **10,** 523–531. doi:10.1038/s41557-018-0023-x. pmid: 29581486 (May 2018).

92. Oeller, M., Sormanni, P. & Vendruscolo, M. An Open-Source Automated PEG Precipitation Assay to Measure the Relative Solubility of Proteins with Low Material Requirement. *Scientific Reports* **11,** 21932. doi:10.1038/s41598-021-01126-4 (1 Nov. 9, 2021).

93. Erkamp, N. A. *et al.* Multidimensional Protein Solubility Optimization with an Ultrahigh-Throughput Microfluidic Platform. *Analytical Chemistry.* doi:10.1021/acs.analchem.2c05495 (Mar. 17, 2023).

94. Dias, C. L. *et al.* The Hydrophobic Effect and Its Role in Cold Denaturation. *Cryobiology. Special Issue: Thermodynamic Aspects of Cryobiology* **60,** 91–99. doi:10.1016/j.cryobiol.2009.07.005 (Feb. 1, 2010).

95. Ikenoue, T. *et al.* Cold Denaturation of α-Synuclein Amyloid Fibrils. *Angewandte Chemie* **126,** 7933–7938. doi:10.1002/ange.201403815 (2014).

96. Noji, M. *et al.* Breakdown of Supersaturation Barrier Links Protein Folding to Amyloid Formation. *Communications Biology* **4,** 120. doi:10.1038/s42003-020-01641-6 (1 Dec. 2021).

97. Mason, T. O. *et al.* Thermodynamics of Polypeptide Supramolecular Assembly in the Short-Chain Limit. *Journal of the American Chemical Society* **139,** 16134–16142. doi:10.1021/jacs.7b00229 (Nov. 15, 2017).

98. Kardos, J., Yamamoto, K., Hasegawa, K., Naiki, H. & Goto, Y. Direct Measurement of the Thermodynamic Parameters of Amyloid Formation by Isothermal Titration Calorimetry*. *Journal of Biological Chemistry* **279,** 55308–55314. doi:10.1074/jbc.M409677200 (Dec. 31, 2004).

99. Van Gils, J. H. M. *et al.* The Hydrophobic Effect Characterises the Thermodynamic Signature of Amyloid Fibril Growth. *PLOS Computational Biology* **16** (ed Dokholyan, N. V.) e1007767. doi:10.1371/journal.pcbi.1007767 (5 May 4, 2020).

100. Mahmoudinobar, F., Urban, J. M., Su, Z., Nilsson, B. L. & Dias, C. L. Thermodynamic Stability of Polar and Nonpolar Amyloid Fibrils. *Journal of Chemical Theory and Computation* **15**, 3868–3874. doi:10.1021/acs.jctc.9b00145 (June 11, 2019).

101. Urbic, T. & Dias, C. L. Thermodynamic Properties of Amyloid Fibrils: A Simple Model of Peptide Aggregation. *Fluid Phase Equilibria* **489**, 104–110. doi:10.1016/j.fluid.2019.02.002 (June 15, 2019).

102. Meisl, G. *et al.* Molecular Mechanisms of Protein Aggregation from Global Fitting of Kinetic Models. *Nature Protocols* **11**, 252–272. doi:10.1038/nprot.2016.010 (2 Feb. 2016).

103. Cohen, S. I. A. *et al.* A Molecular Chaperone Breaks the Catalytic Cycle That Generates Toxic Aβ Oligomers. *Nature Structural & Molecular Biology* **22**, 207–213. doi:10.1038/nsmb.2971 (3 Mar. 2015).

104. Törnquist, M. *et al.* Ultrastructural Evidence for Self-Replication of Alzheimer-associated Aβ42 Amyloid along the Sides of Fibrils. *Proceedings of the National Academy of Sciences* **117**, 11265–11273. doi:10.1073/pnas.1918481117 (May 26, 2020).

105. Trumbore, C. N. & Raghunandan, A. An Alzheimer's Disease Mechanism Based on Early Pathology, Anatomy, Vascular-Induced Flow, and Migration of Maximum Flow Stress Energy Location with Increasing Vascular Disease. *Journal of Alzheimer's Disease* **90**, 33–59. doi:10.3233/JAD-220622 (Jan. 1, 2022).

106. Gomes, L. *et al.* 96-Well Microtiter Plates for Biofouling Simulation in Biomedical Settings. *Biofouling* **30**, 535–546. doi:10.1080/08927014.2014.890713. pmid: 24684538 (May 28, 2014).

107. Scheres, S. H. W., Ryskeldi-Falcon, B. & Goedert, M. Molecular Pathology of Neurodegenerative Diseases by Cryo-EM of Amyloids. *Nature* **621**, 701–710. doi:10.1038/s41586-023-06437-2 (Sept. 2023).

108. *Definition of POLY* https://www.merriam-webster.com/dictionary/poly (2024).

Printed by Tryckeriet i E-huset, Lund 2024

LUND UNIVERSITY

Doctoral Thesis
ISBN 978-91-8096-074-8 (print)
ISBN 978-91-8096-075-5 (pdf)